NATIONAL ADVISORY COMMITTEE FOR AERONAUTICS

TECHNICAL NOTE 2453

AN EXPERIMENTAL STUDY OF WATER-PRESSURE DISTRIBUTIONS DURING LANDINGS AND PLANING OF A HEAVILY LOADED RECTANGULAR FLAT-PLATE MODEL

By Robert F. Smiley

Langley Aeronautical Laboratory
Langley Field, Va.

Washington
September 1951

NATIONAL ADVISORY COMMITTEE FOR AERONAUTICS

TECHNICAL NOTE 2453

AN EXPERIMENTAL STUDY OF WATER-PRESSURE DISTRIBUTIONS DURING LANDINGS AND PLANING OF A HEAVILY LOADED RECTANGULAR FLAT-PLATE MODEL

By Robert F. Smiley

SUMMARY

As part of a landing investigation being conducted at the Langley impact basin to determine the distribution of water pressure on seaplanes, a rectangular flat-plate model, 1 foot wide and 5 feet long, was subjected to smooth-water impact and planing tests. Landings were made at fixed trims of 6°, 9°, 12°, 15°, 30°, and 45° for a range of flight-path angles from approximately 2° to 20°, with beam-loading coefficients of 18.8 and 36.5. Planing runs were made at trims of 6°, 15°, 30°, and 45°.

Initial impact conditions and maximum pressures are presented in tables and figures for all impacts, together with time histories of the pressure distribution, draft, vertical velocity, vertical acceleration, and wetted length.

The pressure coefficients based on the equivalent planing velocity appeared to be substantially independent of the deceleration of the model normal to the plate. The peak pressures were substantially equal to the dynamic pressure corresponding to the velocity of the peak-pressure point, for which velocity an approximate equation was derived. For wetted-length - beam ratios greater than approximately 1.5, this velocity was equal to the equivalent planing velocity for all flight-path angles; for wetted-length - beam ratios less than approximately 1.5, the ratio between this velocity and the equivalent planing velocity was unity for planing (0° flight-path angle) and increased with increase of flight-path angle.

INTRODUCTION

In order to obtain information regarding the magnitude and distribution of the hydrodynamic loads occurring during seaplane landings, a

large amount of theoretical and experimental research has been conducted (references 1 to 18), most of which has dealt with the problem of a V-bottom prismatic surface having a finite angle of dead rise (references 1 to 10). For the limiting case of 0° angle of dead rise (the rectangular flat plate), some research has been conducted but the available information is hardly adequate to describe completely all practical conditions.

In order to supply more complete information on this subject, a series of landing and planing tests has been conducted at the Langley impact basin with a rectangular flat-plate model having a beam of 1 foot and a length of 5 feet. Fixed-trim landings were made in smooth water for a large range of trims, velocities, and flight-path angles and for beam-loading coefficients of 18.8 and 36.5. During each landing, time histories of the pressures, velocities, draft, wetted length, and overall loads were recorded. Also, several planing runs were made during which pressure and horizontal-velocity measurements were recorded.

The purpose of this paper is to present the experimental pressure-distribution, velocity, draft, wetted-length, and acceleration data obtained from these landing and planing tests and to analyze these data to show the effects of instantaneous flight-path angle, beam loading or model deceleration, and the velocity of the peak-pressure point on the pressure distribution. The peak pressures are correlated with the dynamic pressure corresponding to the velocity of the peak-pressure point, for which velocity an approximate equation is derived.

SYMBOLS

b	beam of model, feet
$\dot{f}$	equivalent planing velocity, feet per second $\left(\dot{x} + \dot{y} \cot \tau \text{ or } \frac{\dot{z}}{\sin \tau}\right)$
g	acceleration due to gravity, 32.2 feet per second per second
m	mass of model and dropping weight, slugs
n_{i_w}	impact acceleration normal to undisturbed water surface, g units
p	instantaneous pressure, pounds per square inch
$\dot{s}$	instantaneous velocity of model parallel to model longitudinal center line, feet per second $(\dot{x} \cos \tau - \dot{y} \sin \tau)$

t	time after water contact, seconds
V	instantaneous resultant velocity of model, feet per second
W	weight of model and dropping weight, pounds
$\dot{w}$	instantaneous velocity of peak-pressure point (see fig. 11), feet per second $\left(\dot{f}\sqrt{N}\right)$
$\dot{x}$	instantaneous velocity of model parallel to undisturbed water surface, feet per second
y	instantaneous draft of model normal to undisturbed water surface, feet
$\dot{y}$	instantaneous velocity of model normal to undisturbed water surface, feet per second
$\dot{z}$	instantaneous velocity of model normal to model surface, feet per second $(\dot{x} \sin \tau + \dot{y} \cos \tau)$
$\ddot{z}$	instantaneous acceleration of model normal to model surface, feet per second per second
γ	instantaneous flight-path angle relative to undisturbed water surface, degrees $\left(\tan^{-1} \frac{\dot{y}}{\dot{x}}\right)$
ζ	distance forward of step, measured parallel to longitudinal center line of model, feet
η	transverse distance from center line of model, feet
λ	distance forward of step, measured parallel to longitudinal center line of model, beams
λ_d	length of model below undisturbed water surface, beams
λ_p	wetted length based on peak-pressure location (longitudinal distance from step to position of peak pressure), beams
ρ	mass density of water, 1.938 slugs per cubic foot
τ	trim, degrees

Subscripts:

o at water contact

p at peak pressure

Dimensionless variables:

C_{Δ} beam-loading coefficient $\left(\frac{m}{\rho b^3}\right)$

N pressure ratio $\left(\frac{\frac{1}{2}\rho\dot{w}^2}{\frac{1}{2}\rho\dot{f}^2}\right)$

$\frac{p}{\frac{1}{2}\rho\dot{f}^2}$ pressure coefficient based on $\dot{f}$

$\frac{p}{\frac{1}{2}\rho\dot{w}^2}$ pressure coefficient based on $\dot{w}$

APPARATUS

The test model was made from a 5-foot length of a 1-foot-wide American standard structural-steel channel weighing 40 pounds per foot. The outside face of this channel was machined to a smooth surface. A sketch of the model is shown in figure 1.

The investigation was conducted in the Langley impact basin with the test equipment and instrumentation described in reference 16. Accelerations in the vertical direction were measured with two oil-damped strain-gage-type accelerometers having approximately 0.65 of the critical damping. One accelerometer had a range from -12g to 12g and a natural frequency of 120 cycles per second and was recorded by a 0.65 critically damped galvanometer having a natural frequency of 150 cycles per second. The other accelerometer had a range from -8g to 8g and a natural frequency of 105 cycles per second and was recorded by a 0.65 critically damped galvanometer having a natural frequency of 100 cycles per second. Pitching moments were obtained from an electrical strain-gage-type dynamometer. The instants of water contact and exit of the model were determined by means of an electrical circuit completed by

the water. Pressures were measured with 19 gages distributed over the hull bottom as shown in figure 1. Eighteen of these gages had flat diaphragms of $\frac{1}{2}$-inch diameter which were mounted flush with the hull bottom. The other was a bellows-type gage with a $\frac{1}{4}$-inch-diameter indicating surface. Natural frequencies of the pressure gages were several thousand cycles per second and the response of the oscillograph recording system was accurate to slightly more than 1000 cycles per second. A sample record is shown as figure 2.

PRECISION

The instrumentation used in these tests gives measurements that are estimated to be usually accurate within the following limits:

Horizontal velocity:	
Initial values for landings, feet per second	±0.5
Time histories for planing runs, feet per second	±1
Initial vertical velocity, feet per second	±0.2
Draft, feet	±0.03
Model weight, pounds	±2
Vertical acceleration, g	±0.2
Pitching moment about step, percent	±8
Pressure, pounds per square inch	±2 ± 0.1p
Time, seconds	±0.005

The limits for the pressure data take into account random and reading errors for a uniformly distributed pressure on the gage diaphragm. If the pressure were substantially nonuniform over the gage, as was probably the case for some of these experimental data, there would be additional errors dependent on the gage size and response characteristics and on the shape of the pressure-distribution pattern.

TEST PROCEDURE

A series of landing and planing runs was made in smooth water with the model at 0° yaw and roll and at various fixed trims. Twenty-two landings were made with the model loaded to a weight of 1176 pounds, which corresponded to a beam-loading coefficient of 18.8. For these landing runs the model was tested at trims of 6°, 9°, 12°, 15°, 30°, and 45° for a range of flight-path angles from approximately 2° to 20°.

Three landings were made with the model loaded to a weight of 2276 pounds, which corresponded to a beam-loading coefficient of 36.5. These three runs were made at trims of 12°, 15°, and 30°, with flight-path angles of approximately 7°, 8°, and 10°, respectively. During each landing a compressed-air engine (described in reference 16) exerted a vertical lift force on the model equal to its weight so that the model simulated a seaplane with wing lift equal to the weight of the seaplane. Otherwise the model was free to move in the vertical direction. The model was attached to a towing carriage weighing approximately 5400 pounds. Because of this large additional carriage inertia, the model did not slow down significantly (horizontally) during any landing.

The planing runs were made with the model set at a given draft which was maintained throughout each run within the limits of accuracy of the equipment. Each run consisted of three stages (fig. 3): (1) the model and carriage were accelerated by a catapult to a maximum velocity, (2) the carriage and model were decelerated slowly by the water load for a distance of approximately 110 feet, and (3) the carriage and model encountered an arresting gear which decelerated it rapidly to rest. While it is apparent that the velocity was not strictly constant at any time during these runs, during the second stage the horizontal deceleration was less than 0.1g, which is believed to be small enough so that the runs closely represent the steady planing condition.

In order to provide an independent check on the accuracy of the pressure data obtained from these tests, the following procedure was used: The pressure distributions read at the time that pressure gage 14 (fig. 1) reached its maximum value were integrated for several landings to obtain the vertical load and pitching moment about the step. In figure 4 the results of these integrations are compared with the corresponding values obtained from the accelerometer and load-measuring dynamometer. (The dynamometer measured the pitching moment about an axis remote from the step. In order to transfer this moment to the step the accelerometer reading was used.) These independent measurements appear to agree within approximately 12 percent, which is of the same order of magnitude as the accumulative errors in the experimental measurements and in the integration process. Although these results partly substantiate the over-all reliability of these pressure measurements, errors may still exist for the extremely localized pressures in the vicinity of the peak pressure at the low trims, since the integral of such errors would usually be small. Such errors might be introduced by the large size of the pressure gages relative to the area over which the peak pressure acts or by the frequency-response characteristics of the gages. While in general the data show no indication of serious errors due to frequency-response characteristics, the area effect is sometimes significant.

RESULTS

The initial vertical velocities, horizontal velocities, resultant velocities, flight-path angles, trims, and model weights for all landings are presented in table I together with the values of the maximum pressures recorded on each pressure gage. In table II are given instantaneous-pressure-distribution measurements from each landing together with the corresponding measurements of time, draft, vertical velocity, and vertical acceleration. The instantaneous horizontal velocities are essentially the same as the corresponding initial values since the change in horizontal velocity during any impact was small. Each of the pressure distributions given in table II was read at a time when one of the pressure gages registered its maximum pressure. Therefore, this table also furnishes the relation between the wetted length based on the peak-pressure location λ_p and the draft of the model.

Time histories of the horizontal velocity for each planing run are given in figure 3. Planing pressure-distribution measurements are given in table III together with the corresponding instantaneous horizontal velocities. Measurements at different times during each run are arbitrarily designated by different capital letters. For the runs at 6° trim the water line fluctuated slightly relative to the model in such a manner that peak pressures occurred on several pressure gages; the pressure distributions presented were read at such times. For the other trims peak pressures did not definitely occur on any of the pressure gages; therefore the distributions presented were read at arbitrary increments of time.

The peak-pressure data are plotted in figure 5 as the dimensionless pressure-distribution coefficients $\frac{p_p}{\frac{1}{2}\rho \dot{f}^2}$ and $\frac{p_p}{\frac{1}{2}\rho \dot{w}^2}$ and some complete pressure distributions from impact and planing runs are shown in figures 6 to 9. Wetted-length relations are shown in figure 10.

DISCUSSION

The treatment of the impact of rectangular flat plates can be approached most conveniently by a consideration of the two extreme conditions, namely, the case of very large wetted-length - beam ratios and the case of very small wetted-length - beam ratios. The experimental data will be examined first in the light of the theory for very large wetted-length - beam ratios.

Large Wetted-Length - Beam Ratios

In the impact of prismatic surfaces, when the wetted-length - beam ratio is large, the instantaneous pressures are generally assumed to be composed of two terms, one proportional to the square of the component of the model velocity normal to the keel (normal to the plate for the rectangular flat plate) and one proportional to the normal deceleration of the model. If the effect of the normal deceleration be small, as is subsequently shown to be true for the conditions of these tests, planing and impacting flat plates having the same normal velocity $\dot{z}$ and the same geometrical conditions of trim and draft should have the same pressure distribution.

The peak pressure on a planing flat plate is equal to the dynamic pressure corresponding to the planing velocity:

$$p_p = \frac{1}{2} \rho \dot{x}^2 \tag{1}$$

The planing velocity is related to the normal velocity by the relation $\dot{z} = \dot{x} \sin \tau$ (see fig. 11(a)) so that equation (1) can be expressed in terms of the normal velocity as

$$p_p = \frac{1}{2} \rho \left(\frac{\dot{z}}{\sin \tau} \right)^2 \tag{2}$$

According to the preceding discussion the pressures during an impact should, for small deceleration effects, depend only on the normal velocity and the draft and trim, so that equation (2) for the peak pressure during planing should be applicable to the impact case as well. During an impact the quantity $\frac{\dot{z}}{\sin \tau}$ is related to the vertical and horizontal velocities by the relation $\frac{\dot{z}}{\sin \tau} = \dot{x} + \dot{y} \cot \tau$ (see fig. 11(c)) so that equation (2) becomes

$$p_p = \frac{1}{2} \rho (\dot{x} + \dot{y} \cot \tau)^2 \tag{3a}$$

For convenience the quantity $\dot{x} + \dot{y} \cot \tau$, which is seen to be a generalization of the planing velocity for the impact case (compare equations (1) and (3a)), will henceforth be called the equivalent planing velocity

and will be designated by the symbol $\dot{f}$. Thus

$$p_p = \frac{1}{2} \rho \dot{f}^2 \tag{3b}$$

The experimental variation of the pressure coefficient $\frac{p_p}{\frac{1}{2} \rho \dot{f}^2}$ is shown in figure 5. At trims of 12° and greater for wetted-length - beam ratios greater than approximately 1.5, the experimental pressure coefficients are nearly equal to 1, as would be expected from equation (3b). For all wetted lengths at the lower trims of 6° and 9° and for very short wetted lengths $(\lambda_p < 0.2)$ at the trims of 12° and 15° the experimental pressure coefficients are considerably less than the expected value of unity. This discrepancy may be at least partly explained by the fact that the pressure-gage diaphragms were too large to respond accurately to the highly localized peak pressures. However, at the trims of 12° and greater for wetted-length - beam ratios less than approximately 1.5, the peak pressures are sometimes considerably larger than the expected value. As can be seen in figure 6, the nature of this deviation appears to be an increase of the pressure coefficients $\frac{p}{\frac{1}{2} \rho \dot{f}^2}$ with increase of flight-path angle for small wetted-length - beam ratios.

Small Wetted-Length - Beam Ratios

The variation of the experimental data for small wetted-length - beam ratios from the theoretical predictions which are applicable to large wetted-length - beam ratios can be explained, at least qualitatively, by consideration of the relative differences in the over-all flow patterns for small and large wetted-length - beam ratios which are illustrated in figure 11.

The peak pressure on the model occurs near the water surface and is approximately equal to the dynamic pressure corresponding to the velocity of the peak-pressure point relative to the undisturbed water $\dot{w}$. For large wetted-length - beam ratios, the trailing edge of the model is far below the water surface and thus has little influence on the flow pattern near the water surface in front of the plate, so that the water pile-up $(\lambda_p - \lambda_d)$ will be practically independent of the draft (fig. 11(c)). For such cases the velocity of the peak-pressure point is horizontal and is the same as the equivalent planing velocity (fig. 11(c)). For small wetted-length - beam ratios, however, the problem is more complicated

because the trailing edge of the model is near the surface and does considerably influence the water pile-up in front of the model. The water pile-up, rather than being constant as for large wetted-length - beam ratios, tends to be roughly proportional to the draft. The velocity of the peak-pressure point (see $\dot{w}$ in fig. 11(b)) is then greater than the equivalent planing velocity so that a closer approximation for the peak pressure is

$$p_p = \frac{1}{2} \rho \dot{w}^2 = \frac{1}{2} \rho \dot{f}^2 N \tag{4}$$

The pressure ratio N (the ratio between the peak pressures for large and small wetted-length - beam ratios) is given approximately by the equation

$$N = 1 + 2 \cos \tau \left[\frac{\sin \gamma}{\sin(\gamma + \tau)} \left(\frac{d\lambda_p}{d\lambda_d} - 1 \right) \right] + \left[\frac{\sin \gamma}{\sin(\gamma + \tau)} \left(\frac{d\lambda_p}{d\lambda_d} - 1 \right) \right]^2 \tag{5}$$

The derivation of this equation is given in the appendix. The ratio N is seen to be unity for planing or for 0° flight-path angle and to increase with increase of flight-path angle. Also, for large wetted-length - beam ratios (λ_p greater than 1.5) where the water pile-up is independent of the draft so that $\frac{d\lambda_p}{d\lambda_d} = 1$, the ratio reduces to 1 regardless of the flight-path angle.

Plots of the experimental variation of the peak pressures and of the complete pressure distribution, in the form of the new pressure coefficient $\frac{p}{\frac{1}{2} \rho \dot{w}^2}$ corrected for the ratio N, are shown in figures 5 and 7, respectively. The determination of the values of N for these figures is described in the appendix. For the trims of 12° and higher the peak pressures are generally in reasonable agreement with the values predicted by equation (4) (see fig. 5) and there is little variation of the corrected pressure coefficients with the flight-path angle (see fig. 7). Figure 5 shows that at the lower trims and at small wetted-length - beam ratios for trims up to 15° the experimental pressures are smaller than the predicted pressures, presumably because of the large size of the pressure-gage diaphragms.

Effect of Deceleration Normal to the Keel

In order to show the effects of the normal deceleration $\ddot{z}$ of the model, experimental pressure coefficients are superimposed in figure 8 for beam-loading coefficients of 18.8 and 36.5 and for as nearly identical geometrical conditions of wetted length, trim, and flight-path angle as were available. Inasmuch as for different beam loadings and constant 1 g wing lift the relative magnitudes of the decelerations will be different (roughly twice as large for the lighter loading), the good agreement of the data for these two beam loadings indicates that the effect of deceleration is small relative to the accuracy of the experimental measurements. This small effect was to be expected from the approximate theoretical derivation of Wagner (reference 1) which gives the maximum increment of acceleration pressure as $\frac{1}{2}\rho\ddot{z}b$; this quantity for all of the flat-plate landings was less than 0.4 pounds per square inch, which is of the same order of magnitude as the experimental error.

A similar comparison is made in figure 9 between planing data and impact data for a beam-loading coefficient of 18.8 at trims of 6°, 15°, and 30°. (For the impact data in this figure the ratio N is substantially equal to unity.) Since the deceleration effect in steady planing is zero, the good agreement of these data also indicates that for the conditions of these impacts the deceleration effects are small. (Planing runs 31 and 32 from table III have been omitted from this comparison because the pressures for those runs are small relative to the experimental accuracy and because the velocities are so small that buoyant forces may be important.)

CONCLUSIONS

From an analysis of the experimental data obtained during a smooth-water landing and planing investigation of a heavily loaded rectangular flat-plate model, the following conclusions may be drawn:

1. The peak pressures are approximately equal to the dynamic pressure corresponding to the velocity of the peak-pressure point. For wetted-length - beam ratios greater than 1.5 this velocity is equal to the equivalent planing velocity for all flight-path angles; for wetted-length - beam ratios less than 1.5 the ratio between this velocity and the equivalent planing velocity is unity for planing (0° flight-path angle) and increases with increase of flight-path angle. An approximate equation has been derived for this variation.

2. The impact pressure coefficients based on the equivalent planing velocity appear to be substantially independent of the deceleration of the model normal to the plate.

Langley Aeronautical Laboratory
National Advisory Committee for Aeronautics
Langley Field, Va., June 1, 1951

APPENDIX

VELOCITY OF THE PEAK-PRESSURE POINT

The velocity of the peak-pressure point can be determined with the aid of the following sketch:

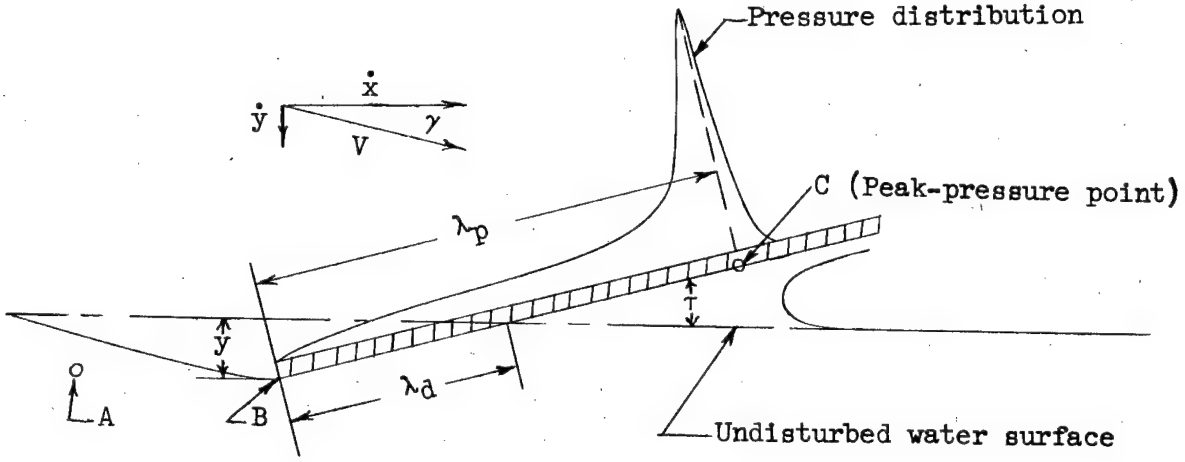

The velocity of the peak-pressure point in space (see $\dot{w}$ in fig. 11(b)) is the resultant of the velocity of the step (point B in the sketch) relative to a fixed point (point A) and the velocity of the peak-pressure point (point C) relative to the step. The horizontal and vertical components of the velocity of the step are $\dot{x}$ and $\dot{y}$, respectively. The horizontal and vertical components of the velocity of the peak-pressure point relative to the step are $\frac{d}{dt}(b\lambda_p \cos \tau)$ and $-\frac{d}{dt}(b\lambda_p \sin \tau)$, respectively. The resultant velocity of the peak pressure point $\dot{w}$ is then

$$\dot{w} = \sqrt{\left[\dot{x} + \frac{d}{dt}\left(b\lambda_p \cos \tau\right)\right]^2 + \left[\dot{y} - \frac{d}{dt}\left(b\lambda_p \sin \tau\right)\right]^2}$$

$$= \sqrt{\left(\dot{x} + b \cos \tau \frac{d\lambda_p}{dt}\right)^2 + \left(\dot{y} - b \sin \tau \frac{d\lambda_p}{dt}\right)^2} \qquad (A1)$$

Assuming that λ_p depends only on λ_d and τ leads to the equation

$$\frac{d\lambda_p}{dt} = \frac{d\lambda_d}{dt}\frac{d\lambda_p}{d\lambda_d} = \frac{\dot{y}}{b \sin \tau}\frac{d\lambda_p}{d\lambda_d} \tag{A2}$$

Combining equations (A1) and (A2) gives

$$\begin{aligned}\dot{w} &= \sqrt{\left(\dot{x} + \dot{y} \cot \tau \frac{d\lambda_p}{d\lambda_d}\right)^2 + \dot{y}^2\left(1 - \frac{d\lambda_p}{d\lambda_d}\right)^2} \\ &= \sqrt{\left[\dot{x} + \dot{y} \cot \tau + \dot{y}\left(\frac{d\lambda_p}{d\lambda_d} - 1\right)\cot \tau\right]^2 + \left[\dot{y}\left(\frac{d\lambda_p}{d\lambda_d} - 1\right)\right]^2} \\ &= \sqrt{\left[\dot{f} + \dot{y}\left(\frac{d\lambda_p}{d\lambda_d} - 1\right)\cot \tau\right]^2 + \left[\dot{y}\left(\frac{d\lambda_p}{d\lambda_d} - 1\right)\right]^2}\end{aligned} \tag{A3}$$

From an examination of figure 11 it can be seen that $\dot{f}$ and $\dot{y}$ are related by the equation $\dot{y} = \dot{f}\frac{\sin \gamma \sin \tau}{\sin(\gamma + \tau)}$. Substituting this relation into equation (A3) and rearranging the terms gives

$$\begin{aligned}\dot{w} &= \dot{f}\sqrt{1 + 2\frac{\sin \gamma}{\sin(\gamma + \tau)}\left(\frac{d\lambda_p}{d\lambda_d} - 1\right)\cos \tau + \left[\frac{\sin \gamma}{\sin(\gamma + \tau)}\left(\frac{d\lambda_p}{d\lambda_d} - 1\right)\right]^2} \\ &= \dot{f}\sqrt{N}\end{aligned} \tag{A4}$$

The dynamic pressure corresponding to this velocity is then

$$\frac{1}{2}\rho\dot{w}^2 = \frac{1}{2}\rho\dot{f}^2 N \tag{A5}$$

where

$$N = 1 + 2\frac{\sin\gamma}{\sin(\gamma+\tau)}\left(\frac{d\lambda_p}{d\lambda_d} - 1\right)\cos\tau + \left[\frac{\sin\gamma}{\sin(\gamma+\tau)}\left(\frac{d\lambda_p}{d\lambda_d} - 1\right)\right]^2 \qquad (A6)$$

from which it is seen that the peak-pressure coefficient $\frac{p_p}{\frac{1}{2}\rho\dot{f}^2}$ should increase with increase of flight-path angle.

In order to obtain numerical values of the velocity ratio N, plots were made of the impact data in table II giving the relation between λ_p and λ_d (figs. 10(a) and 10(b)). These curves were graphically differentiated to obtain $\frac{d\lambda_p}{d\lambda_d}$ (fig. 10(c)) which was substituted into equation (A6) together with the flight-path-angle data from tables I and II $\left(\gamma = \tan^{-1}\frac{\dot{y}}{\dot{x}}\right)$. The values of $\dot{x}$, which is approximately equal to $\dot{x}_o$, were taken from table I.

Insomuch as the accurate evaluation of the quantity $\frac{d\lambda_p}{d\lambda_d}$ is rather important in the evaluation of N, some idea of the accuracy with which this quantity can be obtained from the experimental data is desirable. Essentially, the accuracy of $\frac{d\lambda_p}{d\lambda_d}$ depends on the precision with which the small difference between the large quantities λ_p and λ_d can be determined. Since λ_d is obtained by dividing the draft by the sine of the trim $\left(\lambda_d = \frac{y}{b\sin\tau}\right)$, the draft measurement is extremely critical, especially at the low trims. Consequently, to obtain an independent check on the draft measurements the accelerometer readings were integrated to determine the draft:

$$y = \dot{y}_o t - \int_0^t \int_0^t n_{i_w} g \, dt \, dt \qquad (A7)$$

Values so obtained for the data for 6° trim are given in table II and the corresponding wetted lengths are shown in figure 10(d). This method

is seen to give a larger value of water rise $(\lambda_p - \lambda_d)$ than was obtained from the variable-resistance slide-wire (reference 16) which was used to obtain the draft data presented in figures 10(a), 10(b), and 10(c). At higher trims the differences between the two methods were smaller but the accelerometer value was usually (though not always) somewhat larger. Some uncertainty therefore appears to exist regarding the exact values of λ_d and $\frac{d\lambda_p}{d\lambda_d}$ given in figure 10 and used primarily in figures 5 and 7. Specifically, use of the accelerometer readings would on the average lower the test points for the pressure coefficients $\frac{p}{\frac{1}{2}\rho w^{\cdot 2}}$ in these two figures for large flight-path angles and short wetted lengths. From an over-all point of view, however, none of the conclusions of this paper would be materially changed by the differences shown by the two methods.

REFERENCES

1. Wagner, Herbert: Über Stoss- und Gleitvorgänge an der Oberfläche von Flüssigkeiten. Z.f.a.M.M., Bd. 12, Heft 4, Aug. 1932, pp. 193-215.

2. Wagner, Herbert: Landing of Seaplanes. NACA TM 622, 1931.

3. Pierson, John D.: On the Pressure Distribution for a Wedge Penetrating a Fluid Surface. Preprint No. 167, S.M.F. Fund Paper, Inst. Aero. Sci. (Rep. No. 336, Project No. NR 062-012, Office of Naval Res., Exp. Towing Tank, Stevens Inst. Tech.), June 1948.

4. Pierson, John D., and Leshnover, Samuel: A Study of the Flow, Pressures, and Loads Pertaining to Prismatic Vee-Planing Surfaces. S.M.F. Fund Paper No. FF-2, Inst. Aero. Sci. (Rep. No. 382, Project No. NR 062-012, Office of Naval Res., Exp. Towing Tank, Stevens Inst. Tech.), May 1950.

5. Korvin-Kroukovsky, B. V., and Chabrow, Faye R.: The Discontinuous Fluid Flow Past an Immersed Wedge. Preprint No. 169, S.M.F. Fund Paper, Inst. Aero. Sci. (Rep. No. 334, Project No. NR 062-012, Office of Naval Res., Exp. Towing Tank, Stevens Inst. Tech.), Oct. 1948.

6. Lamb, Horace: Hydrodynamics. Sixth ed., Cambridge Univ. Press, 1932, pp. 94-105.

7. Jones, E. T., and Blundell, R. W.: Force and Pressure Measurements on V-Shapes on Impact with Water Compared with Theory and Seaplane Alighting Results. R. & M. No. 1932, British A.R.C., 1938.

8. Jones, E. T.: Some Measurements of Pressure over a Vee-Shape When Dropped into Water. R. & M. No. 2312, British A.R.C., 1935.

9. Sottorf, W.: Experiments with Planing Surfaces. NACA TM 739, 1934.

10. Smiley, Robert F.: A Study of Water Pressure Distributions during Landings with Special Reference to a Prismatic Model Having a Heavy Beam Loading and a 30° Angle of Dead Rise. NACA TN 2111, 1950.

11. Wagner, Herbert: Planing of Watercraft. NACA TM 1139, 1948.

12. Sottorf, W.: Experiments with Planing Surfaces. NACA TM 661, 1932.

13. Weinig, F.: On the Theory of Hydrofoils and Planing Surfaces. NACA TM 845, 1938.

14. Pierson, John D., and Leshnover, Samuel: An Analysis of the Fluid Flow in the Spray Root and Wake Regions of Flat Planing Surfaces. Preprint No. 166, S.M.F. Fund Paper, Inst. Aero. Sci. (Rep. No. 335, Project No. NR 062-012, Office of Naval Res., Exp. Towing Tank, Stevens Inst. Tech.), Oct. 1948.

15. Cooper, E. P.: Theory of Water Entry of Missiles with Flat Noses. NAVORD Rep. 1154, NOTS 208, U. S. Naval Ordnance Test Station, April 26, 1949.

16. Batterson, Sidney A.: The NACA Impact Basin and Water Landing Tests of a Float Model at Various Velocities and Weights. NACA Rep. 795, 1944.

17. Mayo, Wilbur L.: Analysis and Modification of Theory for Impact of Seaplanes on Water. NACA Rep. 810, 1945.

18. Milwitzky, Benjamin: A Generalized Theoretical and Experimental Investigation of the Motions and Hydrodynamic Loads Experienced by V-Bottom Seaplanes during Step-Landing Impacts. NACA TN 1516, 1948.

TABLE I

INITIAL IMPACT CONDITIONS AND MAXIMUM BOTTOM PRESSURES

Run	τ (deg)	V_o (fps)	γ_o (deg)	$\dot{y}_o$ (fps)	$\dot{x}_o$ (fps)	Maximum pressure (lb/sq in.) at gage - 1	2	3	4	5	6	7	8	9	10	11	12	13	14	15	16	17	18	19
W = 1176 lb; C_Δ = 18.8																								
1	6	80.1	2.1	2.9	80.0	30.3	49.9	50.5	49.1	50.9	46.1	42.6	40.2	(a)	(a)	(a)	(a)	(a)	(a)	(a)	(a)	(a)	(a)	(a)
2		51.9	2.9	2.6	51.9	16.9	31.8	29.9	29.3	32.5	28.2	26.3	26.8	23.0	22.0	21.0	20.2	17.4	22.3	14.6	(a)	(a)	(a)	(a)
3		44.8	3.3	2.6	44.7	13.8	24.2	22.1	24.3	24.4	22.1	21.2	22.1	18.9	18.6	18.6	18.0	16.4	22.5	14.7	(a)	(a)	(a)	(a)
4		44.2	7.6	5.8	43.8	23.5	43.3	41.0	48.3	57.8	43.8	48.0	49.2	43.1	43.5	43.5	43.4	33.4	62.0	45.3	36.0	31.1	37.0	24.5
5	9	86.4	1.8	2.7	86.4	43.5	52.8	55.5	54.5	52.7	40.4	43.3	(a)	(a)	(a)	(a)	(a)	(a)	(a)	(a)	(a)	(a)	(a)	(a)
6		85.9	3.5	5.2	85.7	57.2	70.9	82.5	73.4	85.0	54.9	61.8	70.5	52.7	52.0	45.1	51.3	46.5	43.4	(a)	(a)	(a)	(a)	(a)
7		44.7	5.9	4.6	44.4	20.3	32.1	31.9	34.2	33.9	16.3	24.1	30.9	25.1	26.2	30.1	24.0	23.3	24.4	21.6	16.3	11.6	17.9	(a)
8	12	62.7	4.8	5.2	62.5	38.3	49.6	52.0	47.9	50.2	44.0	44.9	42.2	31.9	31.0	28.9	28.4	28.3	27.0	(a)	(a)	(a)	(a)	(a)
9		61.8	5.0	5.4	61.5	41.0	55.7	52.3	51.2	51.7	45.7	45.9	43.2	34.1	31.9	29.4	29.2	29.5	27.5	(a)	(a)	(a)	(a)	(a)
10		40.5	6.7	4.7	40.2	21.2	30.8	27.5	27.4	29.2	24.1	23.7	23.6	19.3	19.5	17.8	18.2	15.5	18.9	17.0	(a)	(a)	(a)	(a)
11		44.4	9.9	7.6	43.8	30.6	48.3	49.5	46.4	50.9	41.8	44.5	40.4	34.8	36.8	36.0	34.1	32.3	36.5	33.5	24.6	23.1	26.4	13.8
12	15	86.1	2.7	4.1	86.0	61.2	72.5	69.3	60.8	55.3	54.5	52.5	(a)	(a)	(a)	(a)	(a)	(a)	(a)	(a)	(a)	(a)	(a)	(a)
13		62.7	4.5	4.9	62.5	32.8	47.3	45.0	42.2	38.6	38.1	37.3	32.6	(a)	(a)	(a)	(a)	(a)	(a)	(a)	(a)	(a)	(a)	(a)
14		39.6	6.0	4.1	39.3	17.5	22.8	22.1	19.4	18.3	17.2	19.2	14.4	11.1	10.3	10.9	9.4	10.3	4.9	(a)	(a)	(a)	(a)	(a)
15		44.2	10.1	7.7	43.5	30.9	44.8	41.0	38.3	37.3	32.4	34.1	32.5	27.6	27.6	26.8	26.5	26.9	26.0	26.5	18.7	17.8	18.7	(a)
16	30	62.3	3.0	3.2	62.2	35.8	31.3	32.4	28.2	(a)	(a)	(a)	(a)	(a)	(a)	(a)	(a)	(a)	(a)	(a)	(a)	(a)	(a)	(a)
17		62.8	5.8	6.4	62.5	46.9	41.9	41.0	37.1	36.6	34.3	33.9	(a)	(a)	(a)	(a)	(a)	(a)	(a)	(a)	(a)	(a)	(a)	(a)
18		39.7	9.9	6.8	39.1	21.9	20.2	19.6	17.8	18.1	16.5	16.1	15.1	11.6	11.6	11.5	11.5	11.1	8.9	(a)	(a)	(a)	(a)	(a)
19		25.2	21.2	9.1	23.5	13.7	13.2	13.4	12.5	11.7	10.6	11.3	10.6	9.3	8.9	8.3	7.7	7.9	8.7	8.4	6.6	6.9	4.8	(a)
20	45	55.8	5.8	[b]5.6	[b]55.5	31.5	25.7	28.8	24.0	21.6	21.8	20.9	(a)	(a)	(a)	(a)	(a)	(a)	(a)	(a)	(a)	(a)	(a)	(a)
21		39.9	10.0	6.9	39.3	19.1	15.7	15.7	13.7	14.9	14.1	13.0	11.7	4.8	1.5	1.5	2.3	1.7	(a)	(a)	(a)	(a)	(a)	(a)
22		26.7	20.4	9.3	25.0	11.9	9.3	10.2	8.8	8.0	7.6	7.4	7.0	6.9	6.6	6.2	6.9	6.6	5.7	5.5	(a)	(a)	(a)	(a)
W = 2276 lb; C_Δ = 36.5																								
23	12	41.0	7.1	5.1	40.7	18.7	27.2	27.9	26.6	29.2	27.1	26.3	27.3	23.0	24.4	24.4	23.0	23.4	21.5	23.8	19.6	13.3	28.7	14.6
24	15	36.8	8.1	5.2	36.4	17.1	22.4	22.1	21.2	20.8	20.0	19.4	19.1	15.9	17.8	17.2	16.5	16.4	15.5	16.6	14.2	12.3	14.7	6.5
25	30	41.3	10.1	7.2	40.7	24.7	22.7	22.9	20.3	21.0	19.6	18.3	18.9	16.5	17.0	16.7	17.1	15.9	16.3	16.2	9.5	7.4	----	(a)

[a]Pressure zero within experimental error.
[b]Estimated value.

TABLE II

INSTANTANEOUS PRESSURE DISTRIBUTIONS ON THE FLAT-PLATE MODEL DURING LANDINGS

t (sec)	y (ft) (a)	y (ft) (b)	$\dot{y}$ (fps)	n_{i_w} (g)	Pressure (lb/sq in.) at gage -																	
					1	2	3	4	5	6	7	8	9	10	11	12	13	14	15	16	17	18	19
Run 1: τ = 6°; W = 1176 lb; $\dot{y}_o$ = 2.9 fps; $\dot{x}_o$ = 80.0 fps																						
0.007	0.03	0.02	2.8	0.3	2.9	49.2	[c]50.5	-0.6	-0.7	0.5	-0.6	-0.9	0	0	0	0	0	0	0	0	0	0
.017	.06	.05	2.8	.7	0	5.6	2.5	[c]49.1	-0.9	0	-1.0	-.9	0	0	0	0	0	0	0	0	0	0
.029	.08	.08	2.6	.8	-.6	2.3	0	6.1	34.7	[c]46.1	[c]42.6	-.9	0	0	0	0	0	0	0	0	0	0
.071	.15	.16	1.4	.8	0	.5	-1.1	0	2.3	2.9	.8	[c]40.2	0	0	0	0	0	0	0	0	0	0
Run 2: τ = 6°; W = 1176 lb; $\dot{y}_o$ = 2.6 fps; $\dot{x}_o$ = 51.9 fps																						
0.008	0.03	0.02	2.6	0.3	1.8	30.8	[c]29.9	0	0	0	0	0	0	0	0	0	0	0	0	0	0	0
.017	.06	.04	2.5	.5	.9	3.8	2.2	[c]29.3	0	0	-.4	0	0	0	0	0	0	0	0	0	0	0
.027	.08	.07	2.4	.6	1.2	2.0	.9	4.9	20.8	[c]28.2	[c]26.3	0	0	0	0	0	0	0	0	0	0	0
.054	.15	.12	1.9	.6	0	1.0	-.1	1.5	1.9	1.7	1.3	[c]26.8	0	0	0	0	0	0	0	0	0	0
.072	.17	.15	1.7	.6	0	.3	-.2	.3	1.2	.8	.7	3.6	[c]23.0	.3	0	0	0	0	0	0	0	0
.086	.18	.17	1.5	.6	0	0	-.4	0	1.2	.8	.4	2.1	5.0	10.2	10.0	12.0	[c]17.4	0	0	0	0	0
.091	.20	.18	1.4	.6	0	0	-.2	.6	1.5	-.5	.4	2.4	3.9	7.1	6.5	7.5	7.8	[c]22.3	0	0	0	0
.138	.26	.21	.8	.5	0	0	-.2	.9	1.2	0	.2	1.5	2.1	2.2	2.7	3.0	2.6	3.7	[c]14.6	0	0	0
Run 3: τ = 6°; W = 1176 lb; $\dot{y}_o$ = 2.6 fps; $\dot{x}_o$ = 44.7 fps																						
0.010	0.03	0.03	2.6	0.2	0	18.3	[c]22.1	0	0	0	0	0	0	0	0	0	0	0	0	0	0	0
.021	.06	.05	2.5	.4	0	2.4	2.0	[c]24.3	0	0	0	0	0	0	0	0	0	0	0	0	0	0
.030	.09	.08	2.4	.4	0	1.1	.4	3.6	18.9	[c]22.1	[c]21.2	0	0	0	0	0	0	0	0	0	0	0
.056	.15	.13	2.1	.5	0	.5	.4	1.5	2.4	1.4	.9	[c]22.1	0	0	0	0	0	0	0	0	0	0
.073	.18	.16	1.8	.5	0	.3	0	0	1.2	.9	.7	3.4	[c]18.9	0	0	0	0	0	0	0	0	0
.085	.20	.18	1.6	.5	0	0	0	0	.8	.3	.7	2.5	4.2	8.4	8.8	10.2	[c]16.4	0	0	0	0	0
.089	.21	.19	1.6	.5	0	0	0	0	1.2	.6	.5	2.2	3.5	5.5	6.4	5.9	5.9	[c]22.5	0	0	0	0
.123	.24	.23	1.1	.4	0	0	0	0	.8	.6	0	1.2	1.6	1.5	2.4	1.6	1.2	1.3	[c]14.7	0	0	0
Run 4: τ = 6°; W = 1176 lb; $\dot{y}_o$ = 5.8 fps; $\dot{x}_o$ = 43.8 fps																						
0.003	0.02	0.02	5.8	---	1.7	43.0	[c]41.0	0	-0.7	-0.5	-0.4	-0.6	0	0	0	0.8	0	0.7	0.6	0.5	0	0	0
.008	.05	.05	5.8	0.7	-.9	3.6	3.6	[c]48.3	-.7	-1.0	-.4	-.6	0	.3	0	.8	.6	.7	1.1	.9	.7	-.5	.5
.012	.08	.07	5.8	.8	-1.4	2.4	1.6	6.9	[c]57.8	[c]43.8	[c]48.0	-.6	0	.3	0	0	.6	.7	.6	.9	.7	-.9	1.1
.024	.15	.13	5.6	.9	-1.4	----	0	1.4	2.7	2.3	2.1	[c]49.2	0	.3	0	.8	.6	.7	1.1	.9	.7	-.9	1.1
.031	.18	.17	5.5	1.0	-1.4	----	0	.6	1.3	1.3	1.3	6.1	[c]43.1	.3	0	.8	.6	.7	1.1	.9	1.4	-.9	1.1
.034	.20	.19	5.4	1.0	-1.4	----	-.4	0	1.3	1.3	.9	4.1	9.7	18.5	20.5	25.6	[c]33.4	1.4	1.1	1.4	1.4	-.9	1.1
.036	.21	.20	5.3	1.1	-1.9	----	-.4	0	1.7	1.0	.8	3.5	7.8	12.9	13.2	14.7	11.9	[c]62.0	1.1	.9	1.4	-.9	1.1
.043	.24	.23	5.0	1.1	-2.0	----	-.4	0	1.0	.8	.6	2.3	3.2	4.4	4.3	5.8	3.7	7.2	[c]45.3	.9	2.1	-.9	1.6
.059	.32	.30	4.6	1.0	-2.0	----	-.6	0	.7	0	0	.9	1.6	1.8	1.5	2.7	2.0	2.8	3.3	20.7	[c]31.1	0	.5
.062	.33	.31	4.5	1.0	-2.0	----	-.6	0	.7	0	0	.9	1.6	1.8	1.5	2.7	2.0	2.8	3.3	12.2	7.8	[c]37.0	.5
.083	.42	.39	3.8	1.0	-.6	----	-.4	0	0	0	0	0	.5	1.2	1.0	1.5	.6	1.4	1.7	2.3	2.1	2.3	[c]24.5

[a]Values obtained from variable-resistance bridge circuit.
[b]Values obtained from accelerometer integrations.
[c]Maximum reading of gage during landing.

NACA

TABLE II - Continued

INSTANTANEOUS PRESSURE DISTRIBUTIONS ON THE FLAT-PLATE MODEL DURING LANDINGS - Continued

t (sec)	y (ft) (a)	$\dot{y}$ (fps)	n_{i_w} (g)	Pressure (lb/sq in.) at gage - 1	2	3	4	5	6	7	8	9	10	11	12	13	14	15	16	17	18	19
Run 5: $\tau = 9^\circ$; W = 1176 lb; $\dot{y}_o$ = 2.7 fps; $\dot{x}_o$ = 86.4 fps																						
0.009	0.02	2.7	0.6	5.0	44.1	^{c}55.5	-0.6	-0.7	0	0	0	0	0	0	0	1.1	0	0	0	0	0	0
.026	.06	2.4	1.0	1.8	8.4	5.8	^{c}54.5	0	0	0	0	0	0	0	0	1.1	0	0	0	0	0	0
.050	.09	1.8	1.1	-.6	3.4	1.9	8.6	42.2	^{c}40.4	^{c}43.3	0	0	0	0	0	1.1	0	0	0	0	0	0
Run 6: $\tau = 9^\circ$; W = 1176 lb; $\dot{y}_o$ = 5.2 fps; $\dot{x}_o$ = 85.7 fps																						
0.007	0.06	5.2	0.7	7.1	^{c}70.9	^{c}82.5	0	0	0	0	0	0	0	0	0	0	0	0	0	0	0	0
.014	.09	5.1	1.2	2.4	11.8	9.0	^{c}73.4	0	0	0	0	0	0	0	0	0	0	0	0	0	0	0
.021	.12	4.9	1.5	1.2	7.1	4.1	14.8	57.7	^{c}54.9	^{c}61.8	0	0	0	0	0	0	0	0	0	0	0	0
.042	.21	3.9	1.8	.6	2.9	.8	4.0	6.5	6.4	5.3	^{c}70.5	0	0	0	0	0	0	0	0	0	0	0
.061	.27	2.9	1.8	0	1.7	.4	1.7	3.6	3.2	2.7	11.9	^{c}52.7	0	0	0	0	0	0	0	0	0	0
.077	.30	2.0	1.6	0	1.3	0	1.1	2.2	2.2	1.5	7.9	16.1	30.5	28.1	34.5	^{c}46.5	0	0	0	0	0	0
.087	.32	1.5	1.5	0	1.0	0	1.1	1.4	1.6	1.9	5.7	11.7	19.6	17.4	19.9	20.2	^{c}43.4	0	0	0	0	0
Run 7: $\tau = 9^\circ$; W = 1176 lb; $\dot{y}_o$ = 4.6 fps; $\dot{x}_o$ = 44.4 fps																						
0.011	0.05	4.5	0.2	2.5	^{c}32.1	^{c}31.9	0	0	0	0	0	0	0	0	0	0	0	0	0	0	0	0
.019	.09	4.5	.5	1.2	5.0	3.0	^{c}34.2	0	0	0	0	0	0	0	0	0	0	0	0	0	0	0
.027	.12	4.4	.6	1.2	2.9	2.1	6.0	23.8	^{c}16.3	^{c}24.1	0	0	0	0	0	0	0	0	0	0	0	0
.049	.21	4.0	.7	1.2	1.5	.9	1.8	2.9	2.2	1.9	^{c}30.9	0	0	0	0	0	0	0	0	0	0	0
.063	.27	3.6	.7	.6	1.5	1.3	1.2	1.4	1.6	1.5	5.5	^{c}25.1	0	0	0	0	0	0	0	0	0	0
.072	.31	3.3	.8	.6	1.4	.9	1.2	1.4	1.6	1.5	3.6	7.7	14.6	17.0	15.5	^{c}23.3	0	0	0	0	0	0
.075	.31	3.3	.7	.6	1.2	.9	1.2	1.4	1.6	1.2	3.6	6.1	10.1	11.9	9.3	10.8	24.4	0	0	0	0	0
.096	.37	2.8	.7	0	1.0	.4	.6	.7	.5	.8	1.8	3.1	3.6	4.4	3.1	2.8	3.2	^{c}21.6	0	0	0	0
.155	.49	1.4	.6	0	.6	0	.6	.7	.5	.8	1.2	1.5	1.2	2.5	1.6	1.1	.8	2.3	12.8	^{c}11.6	0	0
.171	.49	1.0	.6	0	.6	0	0	.7	.5	.8	1.2	1.5	1.2	1.9	1.6	1.1	.8	1.7	6.2	4.5	^{c}17.9	0

[a]Values obtained from variable-resistance bridge circuit.
[c]Maximum reading of gage during landing.

TABLE II - Continued

INSTANTANEOUS PRESSURE DISTRIBUTIONS ON THE FLAT-PLATE MODEL DURING LANDINGS - Continued

t	y	$\dot{y}$	n_{i_w}	Pressure (lb/sq in.) at gage -																		
(sec)	(ft) [a]	(fps)	(g)	1	2	3	4	5	6	7	8	9	10	11	12	13	14	15	16	17	18	19
Run 8: $\tau = 12^\circ$; W = 1176 lb; $\dot{y}_o = 5.2$ fps; $\dot{x}_o = 62.5$ fps																						
0.008	0.05	5.2	0.5	6.8	[c]49.6	[c]52.0	1.2	0.7	0.5	0	0	0.5	0	0	0	-0.6	0	0	0	0	0.5	0
.019	.09	5.1	1.1	3.1	10.2	7.5	[c]47.9	.7	0	-.9	-.6	0	0	-.5	0	-.6	0	-.6	0	-.6	-.5	0
.028	.14	4.9	1.3	2.5	5.7	4.6	11.5	44.1	[c]44.0	[c]44.9	-.6	0	0	-.5	0	-.6	0	0	0	0	0	0
.056	.25	3.8	1.3	2.5	3.0	2.1	6.4	8.1	7.0	5.4	[c]42.2	1.1	.3	0	.8	-.6	0	0	0	0	.5	0
.081	.33	2.7	1.3	1.2	1.8	1.3	3.5	4.8	4.3	3.2	9.8	[c]31.9	.3	.5	.8	-.6	0	.6	0	0	.5	0
.101	.37	2.1	1.3	1.2	1.6	.8	3.5	4.1	3.2	2.3	5.8	12.2	22.0	22.3	24.5	[c]28.3	.8	0	.4	.6	.5	.5
.111	.39	1.5	1.2	1.2	1.4	.8	2.3	4.1	2.7	2.3	5.2	9.6	14.8	14.7	15.3	14.7	[c]27.0	.6	0	.6	.5	1.1
Run 9: $\tau = 12^\circ$; W = 1176 lb; $\dot{y}_o = 5.4$ fps; $\dot{x}_o = 61.5$ fps																						
0.008	0.03	5.3	0.5	6.3	50.9	[c]52.3	0	0.7	0	0	0	0	0	0	0	0.6	0	0	0	0	0	0
.017	.09	5.3	.8	2.4	10.5	8.2	[c]51.2	0	0	-.9	0	0	0	0	0	.6	0	0	0	.7	-.5	.5
.028	.14	5.0	1.1	1.8	6.0	4.3	11.4	43.3	[c]45.7	[c]45.9	0	0	0	0	0	.6	0	0	0	.7	0	.5
.057	.24	3.8	1.2	.6	3.3	2.0	6.5	6.0	6.3	4.7	[c]43.2	0	.3	.5	1.5	.6	1.1	0	0	1.3	-.5	1.1
.082	.32	2.9	1.2	-.6	2.2	.5	1.5	3.2	3.3	3.1	9.2	[c]34.1	.3	.5	1.5	.6	1.1	.6	0	1.3	-.9	1.1
.099	.36	2.2	1.2	-.3	2.2	-.2	.9	2.5	3.0	2.2	6.2	11.9	22.5	21.5	24.7	[c]29.5	2.2	1.2	.4	2.0	-.9	1.6
.110	.38	1.6	1.1	-.6	2.0	-.2	.3	2.1	2.5	1.9	5.0	9.9	14.8	14.5	15.7	15.4	[c]27.5	1.2	.9	2.0	-.9	1.6
Run 10: $\tau = 12^\circ$; W = 1176 lb; $\dot{y}_o = 4.7$ fps; $\dot{x}_o = 40.2$ fps																						
0.009	0.05	4.7	0.4	1.3	29.0	[c]27.5	0	0.7	0.6	0	0	0	0	0	0	0.5	0	0	0	0	0	0
.021	.11	4.7	.6	0	4.8	4.2	[c]27.4	0	0	-.5	.6	0	0	0	0	.5	0	1.2	.5	0	0	0
.032	.15	4.5	.7	.6	2.9	2.5	5.5	24.1	[c]24.1	[c]23.7	0	.6	0	0	0	.5	0	0	0	0	0	0
.060	.26	3.8	.8	0	1.6	1.3	1.8	4.4	3.4	2.4	[c]23.6	0	0	.5	0	.5	0	0	0	0	0	0
.079	.34	3.5	.9	-.6	1.2	.8	.6	2.2	1.7	.9	5.0	[c]19.3	0	.5	.8	.5	0	-.6	-.4	0	0	0
.091	.38	3.3	.9	-.6	.8	.8	.6	2.2	1.7	.9	3.1	7.2	13.4	13.5	15.1	[c]15.5	0	-.6	0	0	0	0
.096	.40	3.0	.8	-.6	.8	.8	1.2	2.2	1.7	.9	3.1	5.5	8.6	9.2	10.3	8.6	[c]18.9	-.6	0	0	0	.6
.129	.46	2.2	.8	-1.3	.7	.8	.6	2.2	1.7	.5	1.2	2.2	3.4	3.8	4.0	3.2	4.0	[c]17.0	.5	0	0	.6
Run 11: $\tau = 12^\circ$; W = 1176 lb; $\dot{y}_o = 7.6$ fps; $\dot{x}_o = 43.8$ fps																						
0.006	0.05	7.6	0.6	5.9	41.1	[c]49.5	.6	0.8	0.5	0	0	0	0	0	0	0	0	0	.5	0	0	1.1
.013	.11	7.5	.9	2.9	8.3	7.4	[c]46.4	.8	-.5	-.4	0	0	.3	0	-.8	.6	0	0	.5	0	0	1.1
.020	.17	7.3	1.1	2.4	6.1	4.9	11.8	43.4	[c]41.8	[c]44.5	-.6	0	0	-.5	-.8	-.6	0	0	.5	0	-.5	.5
.035	.29	6.8	1.3	.6	2.6	2.5	3.4	5.5	5.7	4.7	[c]40.4	0	0	0	0	.6	0	0	.5	0	0	1.1
.045	.35	6.6	1.4	0	2.4	1.6	2.8	3.9	3.7	3.1	9.4	[c]34.8	0	-.5	.8	.6	0	0	.5	0	.5	.5
.051	.38	6.4	1.4	0	2.3	1.2	2.3	3.9	3.1	2.7	6.4	12.7	24.3	24.5	26.3	[c]32.3	0	0	.5	.7	.5	1.1
.053	.40	6.3	1.4	0	2.1	1.2	1.7	3.2	2.6	2.3	5.9	10.5	18.0	17.7	17.8	18.1	[c]36.5	0	.5	.7	.5	1.6
.066	.48	5.6	1.4	-.6	1.7	.4	1.1	2.4	2.1	1.6	2.9	4.4	6.6	6.3	6.2	5.7	7.5	[c]33.5	.5	0	.9	1.6
.098	.61	4.4	1.4	-1.2	1.5	-.4	.6	0	.5	.4	1.2	1.1	3.0	2.1	2.3	2.8	4.3	5.6	23.7	[c]23.1	1.4	2.1
.104	.64	4.1	1.3	-1.2	1.3	-.4	-.6	.8	1.0	.8	1.2	1.7	3.0	2.6	3.9	2.3	4.3	5.6	13.7	14.7	[c]26.4	2.1
.160	.80	2.1	1.0	-1.8	-1.1	-1.2	-1.1	-.8	0	0	.6	.6	1.5	1.6	2.3	1.1	2.1	2.8	2.7	4.2	1.4	[c]13.8

[a] Values obtained from variable-resistance bridge circuit.
[c] Maximum reading of gage during landing.

TABLE II - Continued

INSTANTANEOUS PRESSURE DISTRIBUTIONS ON THE FLAT-PLATE MODEL DURING LANDINGS - Continued

t (sec)	y (ft) (a)	$\dot{y}$ (fps)	n_{i_w} (g)	Pressure (lb/sq in.) at gage - 1	2	3	4	5	6	7	8	9	10	11	12	13	14	15	16	17	18	19
Run 12: $\tau = 15^\circ$; W = 1176 lb; $\dot{y}_o = 4.1$ fps; $\dot{x}_o = 86.0$ fps																						
0.012	0.06	4.0	0.9	11.3	66.3	[c]69.3	0.6	0	0.5	0	0	0.5	0	0	0	0	0	0	0	0	-0.5	-0.5
.028	.13	3.7	1.5	5.4	17.3	13.6	[c]60.8	0	1.1	0	0	0	0	0	0	0	0	.6	0	0	-.5	-.5
.048	.19	2.7	1.8	4.2	10.2	7.6	19.9	53.1	[c]54.5	[c]52.5	.6	0	-.3	0	0	0	0	.6	0	0	-.5	-.5
Run 13: $\tau = 15^\circ$; W = 1176 lb; $\dot{y}_o = 4.9$ fps; $\dot{x}_o = 62.5$ fps																						
0.009	0.06	4.9	0.6	6.8	[c]47.3	[c]45.0	0.6	0.7	1.0	0	0	0	0	0	0	0	0	0	0	0	0	0
.023	.12	4.8	1.1	4.2	11.8	9.3	[c]42.2	.7	1.0	0	0	0	0	0	0	0	0	0	0	0	0	0
.037	.19	4.4	1.2	3.1	7.3	6.0	13.9	[c]38.6	[c]38.1	[c]37.3	0	0	0	0	0	0	0	0	0	0	0	0
.088	.31	2.3	1.3	2.6	3.2	2.4	3.9	6.0	6.3	4.4	[c]32.6	0	0	0	-.7	0	0	0	0	0	0	.5
Run 14: $\tau = 15^\circ$; W = 1176 lb; $\dot{y}_o = 4.1$ fps; $\dot{x}_o = 39.3$ fps																						
0.014	0.06	4.1	0.3	3.1	21.6	[c]22.1	0	0	0	0	0	0	0	0	0	0	0	0	0	0	0	0
.030	.12	3.9	.5	.6	5.1	3.8	[c]19.4	0	0	-.5	0	0	0	0	0	0	0	0	0	0	0	0
.045	.18	3.7	.6	.6	3.0	2.1	4.8	18.2	[c]17.2	[c]19.2	0	0	.3	-.6	0	0	0	0	0	0	0	0
.094	.34	2.6	.7	0	1.5	1.3	1.2	2.8	2.8	3.2	[c]14.4	0	.3	.6	0	0	0	0	0	0	0	0
.135	.43	1.6	.7	0	0	.4	1.2	2.1	1.1	1.8	5.5	[c]11.1	.3	.6	0	0	0	0	0	0	0	0
.174	.48	.8	.6	0	0	0	0	1.4	.6	1.4	3.6	5.5	9.5	10.3	11.8	[c]10.3	0	0	0	0	0	0
.220	.51	0	.4	-1.3	-.6	-.4	0	-.7	-.6	.5	1.8	3.8	6.4	7.3	7.8	7.4	[c]4.9	.6	.4	.7	-.5	1.1
Run 15: $\tau = 15^\circ$; W = 1176 lb; $\dot{y}_o = 7.7$ fps; $\dot{x}_o = 43.5$ fps																						
0.006	0.06	7.6	0.4	6.0	37.7	[c]41.0	0	0	0	-0.4	0	0	0	0	0	0	0	-0.5	0	0	0	0
.014	.12	7.5	.8	3.0	10.9	7.6	[c]38.3	0	.5	-1.3	0	0	0	0	0	0	0	0	0	0	0	0
.021	.18	7.4	1.0	1.8	5.7	4.8	10.8	32.3	[c]32.4	[c]34.1	.6	0	.3	0	.8	0	0	0	0	0	0	0
.041	.32	6.7	1.3	1.2	3.3	2.8	4.0	5.3	5.7	4.8	[c]32.5	0	.3	0	.8	0	0	0	0	0	0	0
.054	.40	6.2	1.4	1.2	2.7	2.4	3.4	4.0	4.1	3.5	10.8	[c]27.6	.3	.5	1.5	0	0	0	0	0	0	0
.062	.44	5.8	1.4	1.2	2.3	2.4	2.9	3.3	3.6	3.1	7.4	13.2	22.7	22.8	25.5	[c]26.9	0	0	0	0	0	0
.065	.47	5.7	1.4	1.2	2.2	2.4	2.9	3.3	3.6	3.1	6.8	10.6	16.1	16.7	17.2	16.6	[c]26.0	.6	0	0	0	0
.084	.55	5.0	1.4	.6	1.7	1.2	2.3	2.6	2.6	2.2	4.5	5.6	6.8	6.6	7.5	5.0	7.9	[c]26.5	0	.7	0	0
.130	.73	3.0	1.3	.6	1.0	.8	1.1	2.0	1.5	1.3	2.8	3.0	3.1	3.0	3.8	1.7	3.1	4.5	18.2	[c]17.8	.5	0
.141	.76	2.6	1.2	0	1.0	.8	.6	1.3	1.0	.9	2.3	2.5	2.6	3.0	3.0	1.1	2.4	3.9	10.4	12.0	[c]18.7	0

[a]Values obtained from variable-resistance bridge circuit.
[c]Maximum reading of gage during landing.

TABLE II - Continued

INSTANTANEOUS PRESSURE DISTRIBUTIONS ON THE FLAT-PLATE MODEL DURING LANDINGS - Continued

t (sec)	y (ft) (a)	$\dot{y}$ (fps)	n_{i_w} (g)	Pressure (lb/sq in.) at gage - 1	2	3	4	5	6	7	8	9	10	11	12	13	14	15	16	17	18	19
Run 16: τ = 30°; W = 1176 lb; $\dot{y}_o$ = 3.2 fps; $\dot{x}_o$ = 62.2 fps																						
0.028	0.09	3.1	0.7	10.2	30.5	[c]32.4	1.1	0	0	0.5	0	0	0	0	0	0	0	0	0	0	0	0
.077	.19	1.8	1.1	6.8	14.9	14.3	[c]28.2	0	0	.5	0	0	0	0	0	0	0	0	0	0	0	0
Run 17: τ = 30°; W = 1176 lb; $\dot{y}_o$ = 6.4 fps; $\dot{x}_o$ = 62.5 fps																						
0.015	0.09	6.2	0.8	13.6	[c]41.9	[c]41.0	1.2	0.8	0	1.2	0	0	0	0	0	0	0	0	0	0	0	0
.034	.21	5.8	1.2	8.0	21.4	18.1	[c]37.1	.8	1.1	2.5	0	0	0	0	0	0	0	0	0	0	0	0
.054	.30	5.0	1.5	4.9	14.6	13.2	23.1	[c]36.6	[c]34.3	[c]33.9	0	0	0	0	0	0	0	0	0	0	0	0
Run 18: τ = 30°; W = 1176 lb; $\dot{y}_o$ = 6.8 fps; $\dot{x}_o$ = 39.1 fps																						
0.013	0.09	6.8	0.4	6.2	19.4	[c]19.6	0.6	0	0	0	0	0	0	0	0	0	0	0	0	0	0	0
.030	.21	6.5	.7	3.9	8.9	9.0	[c]17.8	0	0	-1.5	0	0	0	0	0	0	0	0	0	0	0	0
.047	.33	6.2	1.0	2.8	6.7	6.6	11.1	17.5	[c]16.5	[c]16.1	.6	0	0	0	0	0	0	0	0	0	0	0
.094	.57	4.7	1.3	1.7	4.0	4.1	5.6	7.4	7.5	6.4	[c]15.1	-.5	0	.5	0	0	0	0	0	0	0	0
.140	.72	3.0	1.2	1.1	3.0	2.9	3.9	4.7	5.0	4.5	9.8	[c]11.6	.9	.5	0	0	0	0	0	0	0	0
.169	.78	1.9	1.2	1.1	2.6	2.9	3.9	4.0	4.5	3.7	6.9	9.1	[c]11.6	[c]11.5	[c]11.5	[c]11.1	1.8	0	0	0	0	0
.200	.81	.9	1.1	1.7	2.4	2.5	3.3	3.4	3.5	3.4	5.8	7.1	9.3	9.4	9.2	7.8	[c]8.9	0	0	0	0	0
Run 19: τ = 30°; W = 1176 lb; $\dot{y}_o$ = 9.1 fps; $\dot{x}_o$ = 23.5 fps																						
0.013	0.10	9.0	0.3	5.4	[c]13.2	[c]13.4	0	0	0	0	0	0	0	0	0	0	0	0	0	0	0	0
.026	.23	8.9	.4	3.6	6.4	5.6	[c]12.5	0	0	0	0	0	0	0	0	0	0	0	0	0	0	0
.037	.34	8.8	.6	2.4	4.5	4.8	7.4	[c]11.7	[c]10.6	[c]11.3	0	0	0	0	0	0	0	0	0	0	0	0
.068	.59	8.2	.8	1.8	3.1	3.0	4.0	5.8	4.8	4.3	[c]10.6	.5	0	0	0	0	0	0	0	0	0	0
.087	.75	7.7	.9	1.8	2.6	2.6	3.4	4.4	3.7	3.5	6.4	[c]9.3	.6	.5	0	0	0	0	0	0	0	0
.096	.82	7.6	.9	1.8	2.6	2.6	2.9	4.4	3.7	3.1	5.3	8.2	[c]8.9	[c]8.3	[c]7.7	[c]7.9	1.9	0	0	0	0	0
.102	.87	7.3	.9	1.8	2.4	2.2	2.9	4.4	3.2	2.7	4.7	7.1	8.3	7.8	7.7	7.4	[c]8.7	0	0	0	0	0
.127	1.04	6.4	1.0	1.2	2.2	2.2	2.9	4.4	2.7	2.7	4.1	4.4	5.0	4.7	3.8	3.4	4.8	[c]8.4	0	0	0	0
.186	1.35	4.8	.9	1.2	1.8	1.7	1.7	2.9	2.1	2.0	2.3	2.7	3.0	2.6	2.3	2.3	2.9	3.9	6.1	[c]6.9	3.1	0
.196	1.40	4.3	.9	.6	1.6	.4	1.7	2.2	1.6	1.6	2.3	2.7	2.7	2.1	2.3	1.7	1.9	3.4	5.7	5.5	[c]4.8	0

[a]Values obtained from variable-resistance bridge circuit.
[c]Maximum reading of gage during landing.

TABLE II - Continued

INSTANTANEOUS PRESSURE DISTRIBUTIONS ON THE FLAT-PLATE MODEL DURING LANDINGS - Continued

t (sec)	y (ft) [a]	$\dot{y}$ (fps)	n_{i_w} (g)	Pressure (lb/sq in.) at gage -																
				1	2	3	4	5	6	7	8	9	10	11	12	13	14	15	16	17	18	19
Run 20: $\tau = 45^\circ$; W = 1176 lb; $\dot{y}_o = 5.6$ fps; $\dot{x}_o = 55.5$ fps																						
0.022	----	---	---	12.3	24.5	[c]28.8	0	0	-0.6	-0.4	0	0	0	0	0	0	0	0	0	0	0	0
.056	----	---	---	9.3	20.8	18.9	[c]24.0	0	-.6	-.4	0	0	0	0	0	0	0	0	0	0	0	0
.093	----	---	---	8.0	15.9	14.9	22.8	[c]21.6	[c]21.8	[c]20.9	0	0	0	0	0	0	0	0	0	0	0	0
Run 21: $\tau = 45^\circ$; W = 1176 lb; $\dot{y}_o = 6.9$ fps; $\dot{x}_o = 39.3$ fps																						
0.023	0.15	6.6	0.3	8.6	[c]15.7	[c]15.7	-1.2	0	0	-1.6	0	0	0	0	0	0	0	0	0	0	0	0
.049	.33	6.3	.7	5.6	11.4	11.1	[c]13.7	0	0	-1.2	0	0	0	0	0	0	0	0	0	0	0	0
.074	.49	5.7	.9	4.3	9.0	8.1	11.7	[c]14.9	[c]14.1	[c]13.0	0	0	0	0	0	0	0	0	0	0	0	0
.159	.83	2.8	1.3	3.1	5.7	5.1	7.0	9.7	8.7	7.5	[c]11.7	0	0	0	0	0	0	0	0	0	-.4	0
.216	.94	.8	1.1	2.5	4.7	4.3	5.3	7.6	7.1	5.9	10.0	[c]4.8	[c]1.5	[c]1.5	2.3	1.7	.7	1.2	.9	2.1	-1.3	1.6
Run 22: $\tau = 45^\circ$; W = 1176 lb; $\dot{y}_o = 9.3$ fps; $\dot{x}_o = 25.0$ fps																						
0.018	0.18	9.2	0.2	6.3	[c]9.3	[c]10.2	0	0	0	0	0	0	0	0	0	0	0	0	0	0	0	0
.035	.33	9.1	.4	4.4	7.1	6.2	[c]8.8	0	0	-.8	0	0	0	0	0	0	0	0	0	0	0	0
.051	.46	8.8	.5	3.1	5.8	4.9	7.6	[c]8.0	[c]7.6	[c]7.4	0	0	0	0	0	0	0	0	0	0	0	0
.095	.80	7.9	.8	3.1	4.4	4.0	6.4	6.9	6.5	5.4	[c]7.0	0	0	0	0	0	0	0	0	0	0	0
.125	1.04	7.2	.8	2.5	4.0	3.5	5.3	5.3	5.4	4.2	7.0	[c]6.9	3.9	3.1	3.1	2.8	.7	0	0	0	0	0
.135	1.09	6.9	.9	2.5	3.8	3.5	5.3	4.6	5.4	4.2	6.4	6.9	6.3	5.7	6.1	[c]6.6	2.8	0	-.9	0	0	0
.145	1.15	6.6	.9	2.5	3.6	3.5	4.7	4.6	4.9	3.9	5.8	6.4	6.6	6.2	6.1	6.1	[c]5.7	0	-.9	-.7	0	0
.185	1.38	5.4	.9	1.9	3.2	3.1	4.7	4.6	4.4	3.1	4.6	4.8	5.1	4.6	4.6	4.4	----	[c]5.5	-.4	-.7	0	0

[a]Values obtained from variable-resistance bridge circuit.
[c]Maximum reading of gage during landing.

TABLE II - Concluded

INSTANTANEOUS PRESSURE DISTRIBUTIONS ON THE FLAT-PLATE MODEL DURING LANDINGS - Concluded

t (sec)	y (ft) [a]	$\dot{y}$ (fps)	n_{i_w} (g)	Pressure (lb/sq in.) at gage - 1	2	3	4	5	6	7	8	9	10	11	12	13	14	15	16	17	18	19
Run 23: τ = 12°; W = 2276 lb; $\dot{y}_o$ = 5.1 fps; $\dot{x}_o$ = 40.7 fps																						
0.009	0.06	5.1	0.2	3.9	26.6	[c]27.9	0	0	0	0	0	0	0	0	0	0	0	0	0	0	0	0
.020	.12	5.1	.3	2.2	5.6	4.9	[c]26.6	0	0	0	0	0	0	0	0	0	0	0	0	0	0	0
.028	.15	5.0	.4	1.1	3.4	3.3	6.9	24.2	[c]27.1	[c]26.3	0	0	0	0	0	0	0	0	0	0	0	0
.052	.27	4.8	.4	.6	1.7	1.6	2.1	4.1	3.6	2.6	[c]27.3	0	-.3	0	0	0	0	0	0	0	0	0
.066	.33	4.6	.5	1.1	1.3	1.2	1.6	3.0	2.5	1.9	6.9	[c]23.0	-.3	0	.7	0	0	0	0	0	0	0
.074	.36	4.5	.5	.6	1.3	.8	1.6	2.4	2.0	1.5	5.7	7.8	16.0	16.2	17.6	[c]23.4	0	0	0	0	0	0
.077	.37	4.5	.5	1.1	1.3	1.2	2.1	2.4	2.5	1.5	4.6	6.8	11.7	11.1	11.7	13.0	[c]21.5	0	0	0	0	0
.097	.44	4.1	.5	0	1.3	.8	.5	2.4	2.0	1.1	1.7	2.0	4.3	3.5	3.7	2.7	4.5	[c]23.8	-.9	0	0	0
.134	.58	3.6	.5	0	1.0	.8	1.1	1.2	1.5	.7	1.7	1.5	1.7	1.5	1.5	1.1	.9	2.7	16.6	[c]13.3	0	0
.141	.59	3.4	.5	0	1.0	.4	.5	1.2	1.5	.4	1.1	1.0	1.7	1.5	1.5	0	.9	2.2	8.8	6.4	[c]28.7	----
.197	.73	2.5	.4	0	0	0	0	0	1.0	.4	.6	1.0	1.1	1.0	1.5	1.1	0	.5	1.3	0	4.2	[c]14.6
Run 24: τ = 15°; W = 2276 lb; $\dot{y}_o$ = 5.2 fps; $\dot{x}_o$ = 36.4 fps																						
0.013	0.06	5.0	0.2	2.8	20.3	[c]22.1	-0.5	0	0	0	0	0	0	0	0	0	0	0	0	0	0	0
.025	.12	4.9	.3	.6	4.8	4.4	[c]21.2	.6	0	-.4	0	0	0	0	0	0	0	0	0	0	0	0
.036	.18	4.8	.4	.6	3.0	2.8	6.0	20.2	[c]20.0	[c]19.4	.6	0	0	0	0	0	0	0	0	0	0	0
.066	.31	4.5	.4	0	1.7	.8	1.6	4.2	4.0	2.6	[c]19.1	-.5	0	0	0	0	0	0	0	0	0	0
.084	.40	4.2	.5	-.6	1.5	1.2	.5	3.0	3.0	1.5	5.6	[c]15.9	.3	.5	0	0	0	0	0	0	0	0
.094	.45	4.1	.5	0	1.5	.8	.5	3.0	2.5	1.5	4.5	7.3	14.4	13.7	15.7	[c]16.4	.9	0	0	0	0	0
.099	.45	4.1	.5	0	1.5	.4	.5	2.4	2.5	1.5	3.9	6.3	10.9	10.1	11.2	11.0	[c]15.5	0	0	0	0	0
.123	.55	3.7	.6	-.6	1.1	.4	.5	1.8	2.0	1.1	2.2	2.9	4.3	3.5	4.5	4.4	5.5	[c]16.6	0	0	0	.5
.179	.72	2.8	.5	-.6	.9	.4	0	1.2	2.0	.4	1.7	1.9	2.3	2.0	2.3	2.2	1.8	3.7	13.3	[c]12.3	-.5	1.1
.189	.75	2.7	.5	0	.9	.4	0	1.8	1.5	.7	1.7	1.5	2.3	2.0	2.3	2.2	1.8	2.7	7.1	6.2	[c]14.7	1.1
.309	.94	1.0	.5	0	.6	.4	0	.6	.5	0	.6	1.5	1.4	0	.8	.6	.9	1.1	1.3	.7	2.2	[c]6.5
Run 25: τ = 30°; W = 2276 lb; $\dot{y}_o$ = 7.2 fps; $\dot{x}_o$ = 40.7 fps																						
0.012	0.09	7.2	0.2	7.5	22.1	[c]22.9	-1.7	0	0	0	0	0	0	0	0	0	0	0	0	0	0	0
.028	.21	7.2	.5	4.0	10.7	10.2	[c]20.3	0	0	-1.5	0	0	0	0	0	0	0	0	0	0	0	0
.042	.31	7.1	.6	2.9	7.9	7.2	12.6	[c]21.0	[c]19.6	[c]18.3	0	0	0	0	0	0	0	0	0	0	0	0
.081	.58	6.3	.7	1.7	5.2	4.3	6.6	8.6	8.2	7.9	[c]18.9	-1.0	0	-.5	0	0	0	0	0	0	0	0
.106	.72	5.6	.9	1.2	4.4	3.4	4.9	5.9	6.7	6.0	11.4	[c]16.5	1.7	1.0	1.5	0	0	0	0	0	----	0
.118	.79	5.4	.9	1.2	4.2	3.4	4.4	5.9	6.2	5.2	9.2	12.5	16.7	16.3	16.3	[c]15.9	5.5	0	0	0	----	0
.126	.84	5.1	.9	.6	4.1	2.6	4.4	5.3	5.7	4.9	8.6	10.5	14.7	14.7	14.8	13.7	[c]16.3	0	0	0	----	0
.165	1.01	4.1	1.0	0	3.5	2.6	2.7	4.0	4.6	4.1	6.3	6.5	8.9	8.1	8.9	7.7	10.9	[c]16.2	0	0	----	0
.302	1.28	.6	.7	-1.2	2.7	.9	1.7	2.0	3.1	2.2	2.9	4.0	4.0	4.1	4.5	3.8	5.5	6.5	[c]9.5	[c]7.4	----	0

[a]Values obtained from variable-resistance bridge circuit.
[c]Maximum reading of gage during landing.

TABLE III

INSTANTANEOUS PRESSURE DISTRIBUTIONS ON THE FLAT-PLATE MODEL DURING PLANING

Run	Distribution	τ (deg)	t (sec)	x (fps)	λ_d (beams)	λ_p (beams)	Pressure (lb/sq in.) at gage[a] -																
							1	2	4	5	6	8	9	10	11	12	13	14	15	16	17	18	19
26	A	6	1.028	60.0	1.75	2.00	0	0.6	---	1.5	0.6	1.7	2.2	7.6	8.1	9.8	[b]14.1	-3.6	---	-0.5	-1.7	1.0	0
	B		1.045	61.0		2.13	0	0	---	.8	0	1.1	1.1	5.7	6.6	7.6	5.4	[b]17.0	---	0	-1.7	1.0	.5
	C		1.318	72.5		2.00	0	0	---	1.5	.6	2.3	3.8	10.9	12.2	15.9	[b]23.8	-2.4	---	-.5	-1.7	1.2	.5
	D		1.322	73.0		2.13	0	0	---	1.5	.6	2.3	3.8	10.3	11.2	13.6	16.2	[b]29.2	---	-.5	-1.7	1.2	.5
	E		1.725	80.0		2.13	0	1.2	---	3.1	.6	2.3	6.5	14.2	13.7	13.6	13.0	[b]29.2	---	-.5	0	.8	0
	F		1.809	80.0		2.13	0	1.2	---	3.1	.6	1.7	5.4	10.3	10.1	10.6	8.7	[b]30.4	---	-.9	0	.6	-.5
	G		1.863	80.0		2.13	0	1.2	---	3.1	.6	2.3	5.9	11.2	11.2	11.4	8.7	[b]38.9	---	-.9	0	.8	-.5
	H		2.545	77.0		2.13	-0.6	-1.8	---	.8	-.6	1.7	4.8	9.4	7.6	6.8	4.3	[b]31.6	---	0	0	1.4	7.6
	I		2.599	76.0		2.00	-1.2	-.6	---	0	-.6	2.3	10.2	.3	.5	[b]25.0	[b]17.8	1.2	---	0	0	1.4	7.6
	J		2.767	72.0		1.87	-1.2	1.2	---	2.3	1.1	4.0	[b]28.5	.3	0	0	-2.2	-1.2	---	-.9	0	1.6	5.4
	K		2.810	71.0		2.00	-.9	0	---	0	-.6	2.3	9.7	[b]28.1	[b]27.9	[b]28.8	[b]22.2	1.2	---	0	-.7	1.6	6.5
	L		2.830	70.0		2.13	-.6	-.6	---	.8	0	1.1	5.9	9.7	9.1	9.1	5.4	[b]35.2	---	-.5	-.7	1.4	6.5
27	A	6	1.862	58.0	2.92	3.29	-2.3	-1.1	---	0	0	-0.5	-1.6	0.3	0.5	0.8	----	----	1.1	5.1	----	[b]17.2	----
	B		2.110	59.0		3.29	-2.3	-1.1	---	0	0	-.5	-1.6	.6	.5	.8	----	----	1.6	4.5	----	[b]16.3	----
	C		2.220	58.5		3.29	-2.3	-1.1	---	.7	-.5	-.5	-1.6	.6	.5	.8	----	----	1.6	4.5	----	[b]18.1	----
	D		2.853	57.5		3.29	-1.2	-.6	---	.7	.5	-.5	-1.6	.6	0	.8	----	----	1.6	4.0	----	[b]----	----
	E		3.416	56.5		3.29	-1.7	-.6	---	.7	.5	-.5	-1.6	.3	0	.8	----	----	1.6	4.5	----	[b]15.5	----
	F		3.801	47.5		3.29	-1.2	-.6	---	0	0	-.5	.5	.3	0	0	----	----	1.6	2.5	----	[b]12.0	----
28	A	15	3.060	40.0	1.75	[c]2.20	0.2	1.4	---	1.6	1.2	2.4	2.8	4.7	5.3	5.4	4.0	6.4	0.6	0.5	0.7	----	----
	B		3.760	39.0		[c]2.20	.8	.8	---	1.6	1.2	1.8	2.8	4.7	4.8	5.4	4.0	6.4	.6	.5	.7	----	----
	C		4.560	38.0		[c]2.20	-.4	.2	---	.8	.6	1.8	2.3	4.3	4.2	5.4	4.0	8.6	.6	1.0	1.4	----	----
29	A	15	3.080	40.5	2.92	[c]3.35	-0.8	0.3	1.9	1.0	0.7	0.7	----	2.1	1.6	3.0	2.2	1.8	2.1	5.6	5.3	6.7	0
	B		3.880	39.0		[c]3.35	-.8	-.2	1.3	.2	.2	.7	----	1.8	1.1	3.0	1.7	2.6	2.1	5.6	5.3	5.9	-.5
	C		4.680	37.5		[c]3.35	-.8	-.2	1.3	1.0	.2	.7	----	1.5	.6	1.6	1.2	3.4	1.6	4.8	4.6	6.3	-.5
30	A	30	3.560	31.0	1.75	[c]2.23	----	----	3.5	3.4	2.6	3.7	4.4	5.7	4.7	4.6	4.7	5.1	0	---	0	0	----
	B		4.560	28.6		[c]2.23	----	----	2.8	1.8	1.4	3.1	3.3	4.7	4.2	3.8	4.1	5.1	0	---	0	0	----
	C		6.160	24.6		[c]2.23	----	----	1.5	1.8	1.4	2.5	2.8	3.5	2.6	3.1	3.5	4.4	.6	---	0	-.5	----
31	A	30	2.910	22.0	2.92	[c]3.4	----	2.2	---	3.3	3.1	-2.6	1.3	1.7	.7	0	0	3.9	---	1.3	0.7	3.9	-2.1
	B		3.910	25.0		[c]3.4	----	2.0	---	3.3	3.1	-2.6	1.3	2.0	1.2	0	.8	4.7	---	1.7	1.3	5.2	-2.7
	C		4.910	23.3		[c]3.4	----	2.0	---	1.8	1.5	-3.7	.7	1.7	1.2	.9	1.9	5.4	---	2.6	3.3	3.0	-.5
	D		6.110	20.5		[c]3.4	----	1.8	---	.4	.9	-3.7	.7	1.4	.7	.9	1.9	5.4	---	2.6	3.3	2.1	-.5
	E		7.310	18.4		[c]3.4	----	1.6	---	2.5	2.0	-3.7	0	.8	0	0	.8	3.2	---	.4	0	3.0	-2.7
32	A	45	2.600	17.9	1.75	[c]2.2	0	0.6	0	0	1.1	1.7	1.6	2.1	1.6	2.2	1.6	2.1	1.7	0	0	0	0
	B		3.600	20.4		[c]2.2	0	.6	0	0	1.1	1.7	2.1	2.7	1.6	2.2	2.2	2.8	1.7	0	0	0	0
	C		5.100	19.9		[c]2.2	0	1.2	.6	0	1.1	2.3	2.1	2.7	2.2	2.2	2.2	2.8	1.1	0	0	0	0
	D		6.600	16.8		[c]2.0	0	.6	.6	0	.6	1.7	1.6	1.8	1.6	2.2	1.6	1.4	0	0	0	0	0
	E		8.100	14.1		[c]1.8	0	1.2	.6	.7	.6	1.7	1.1	.9	1.1	.8	.5	0	0	0	0	0	-1.1

[a]Gages 3 and 7 were erratic during all planing runs.
[b]Peak value.
[c]Estimated value.

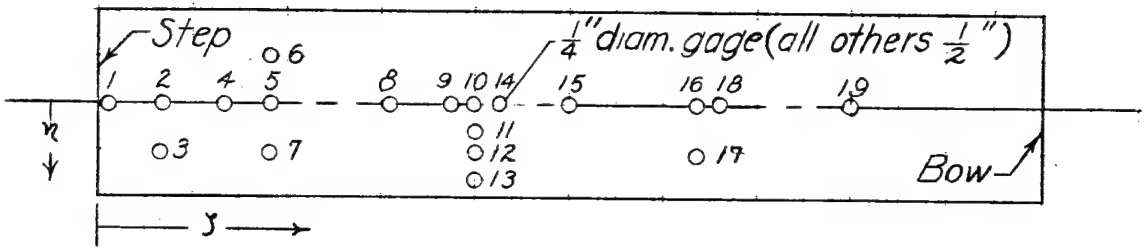

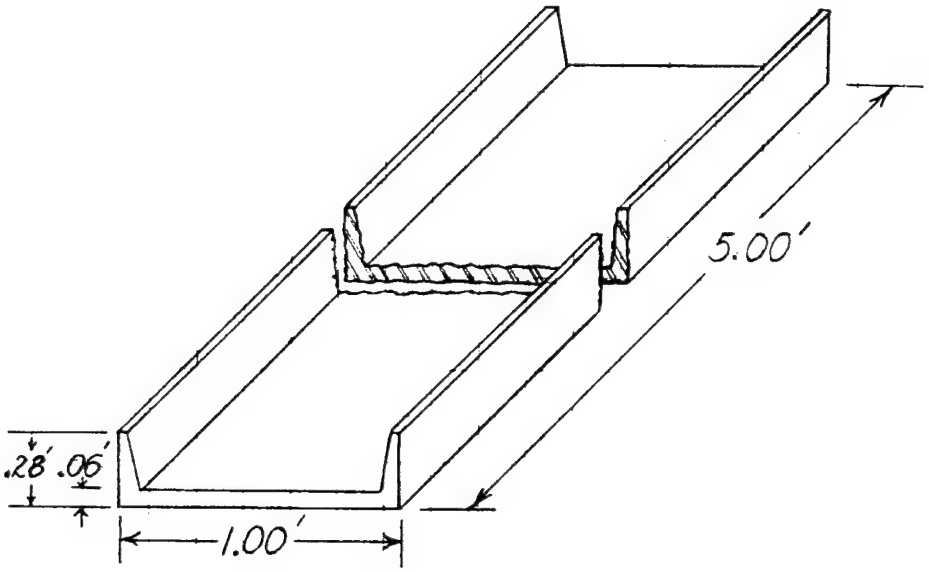

Position	y (ft)	η (ft)	Position	y (ft)	η (ft)
1	0.05	0	11	2.00	0.14
2	.33	0	12	2.00	.27
3	.33	.27	13	2.00	.41
4	.67	0	14	2.13	0
5	.92	0	15	2.50	0
6	.92	-.27	16	3.17	0
7	.92	.27	17	3.17	.27
8	1.54	0	18	3.29	0
9	1.87	0	19	4.00	0
10	2.00	0	Bow	5.00	—

Figure 1.- Hull lines and pressure-gage positions on the flat-plate model.

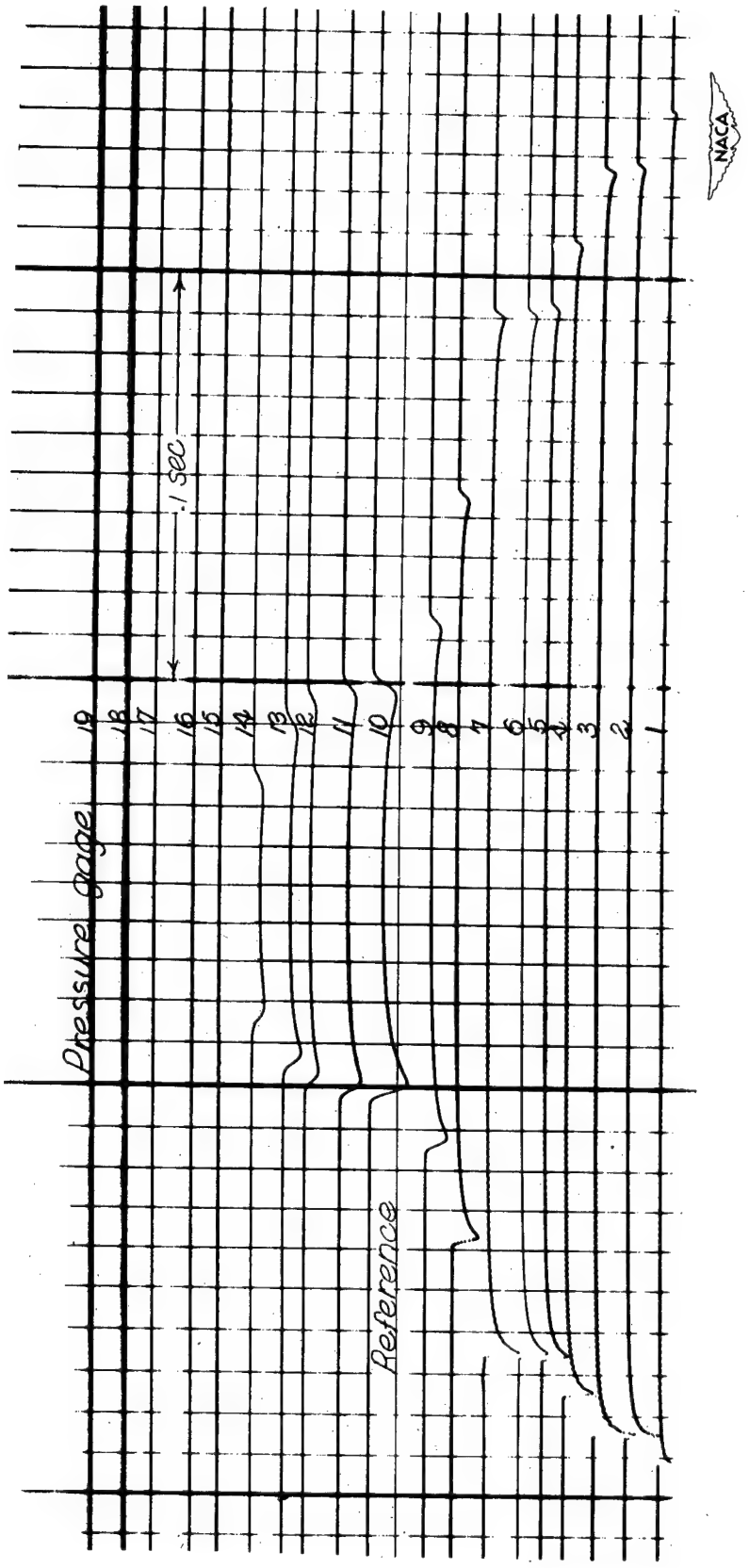

Figure 2.- Sample oscillograph record showing pressure-gage traces. Run 8.

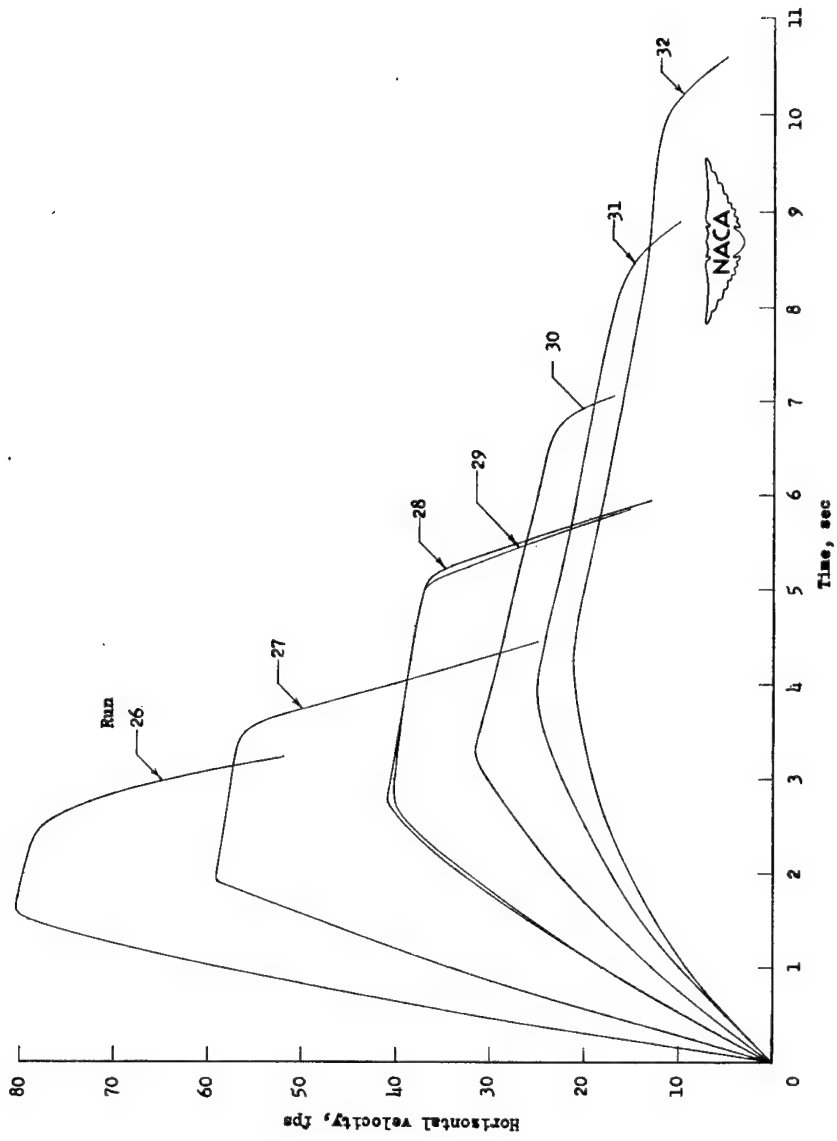

Figure 3.- Horizontal-velocity time histories for the flat-plate planing runs.

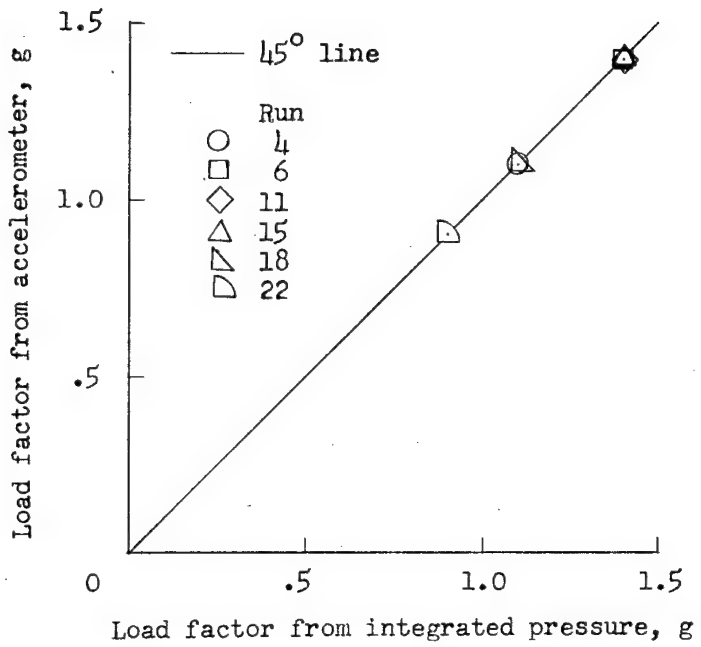

(a) Vertical load factor at time of maximum pressure on gage 14.

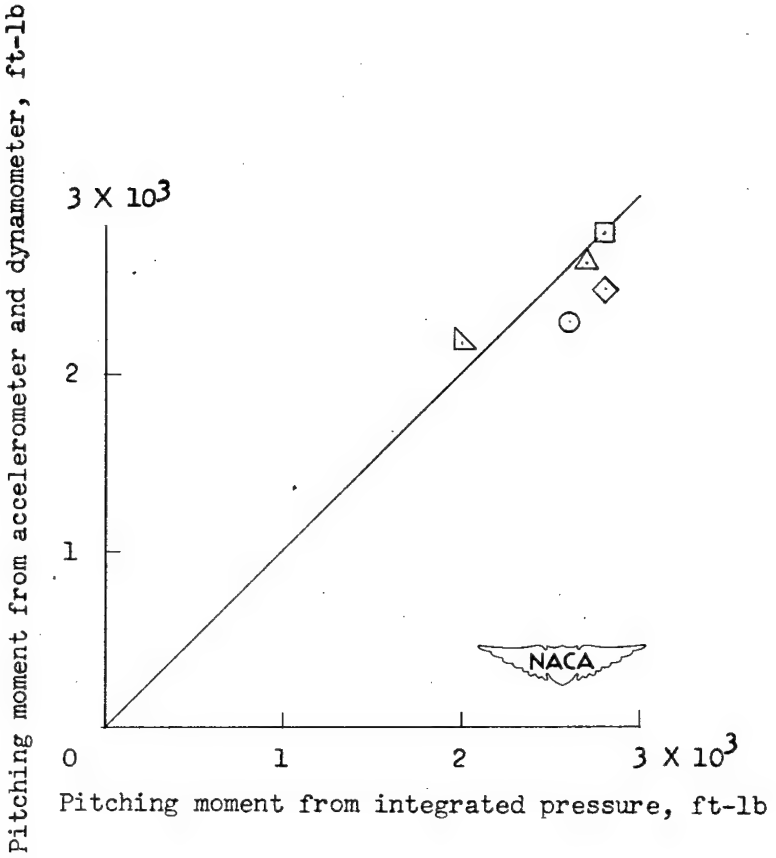

(b) Pitching moment about step at time of maximum pressure on gage 14.

Figure 4.- Comparison of experimental measurements of over-all loads and pitching moments with corresponding values obtained by integration of experimental pressure distributions.

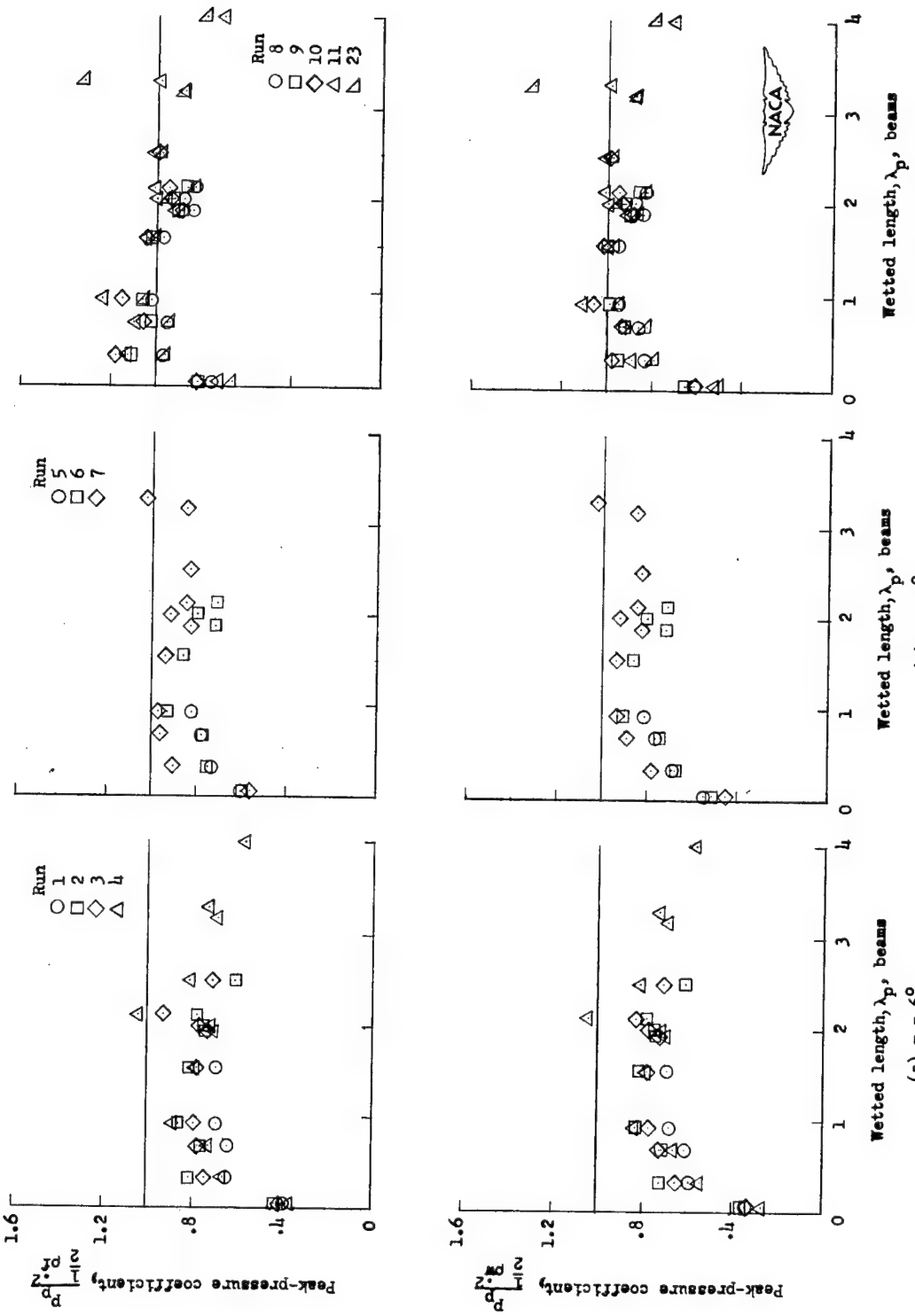

Figure 5.- Experimental peak-pressure coefficients on the flat-plate model for various trims and wetted lengths.

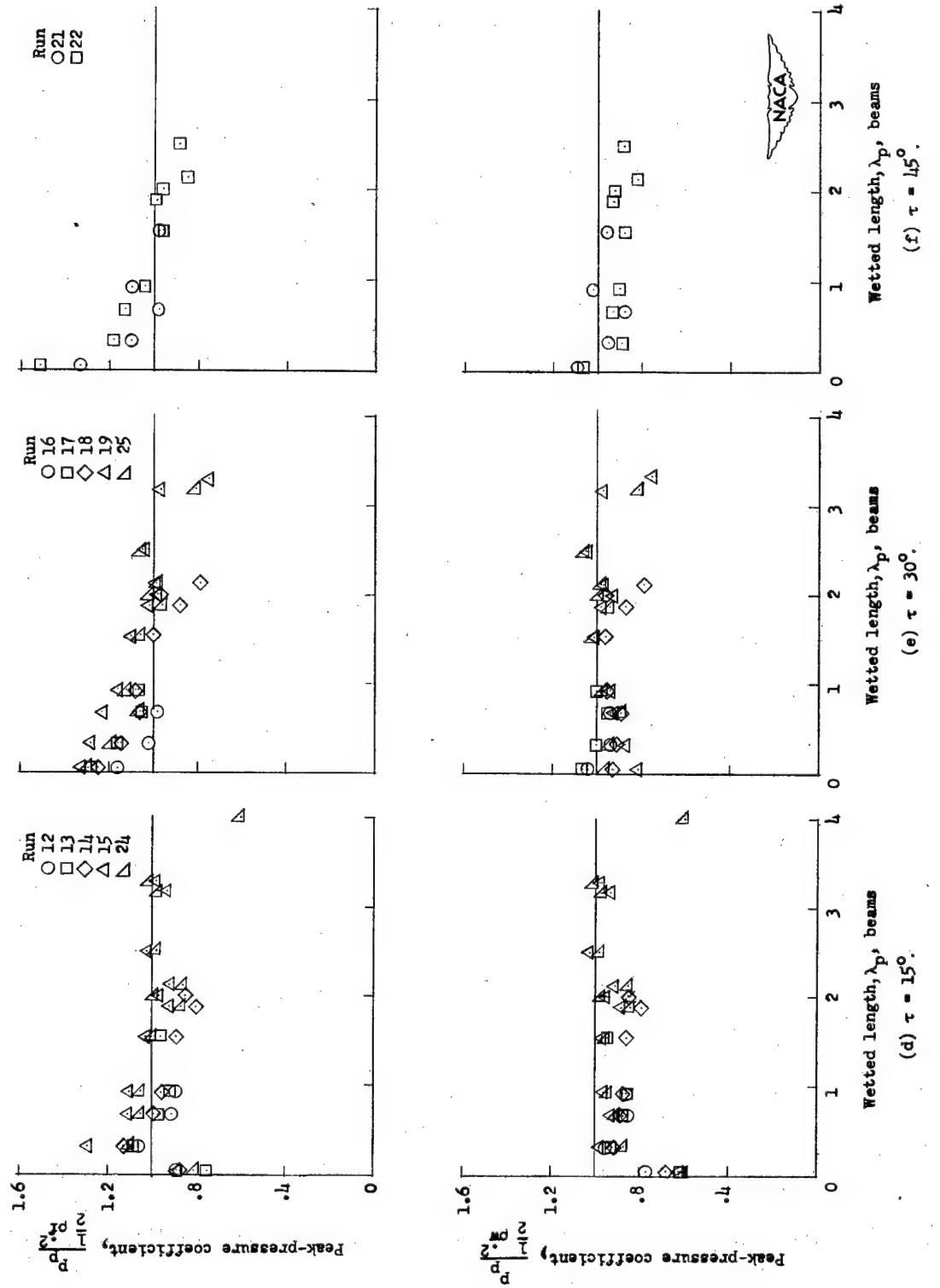

Figure 5.- Concluded.

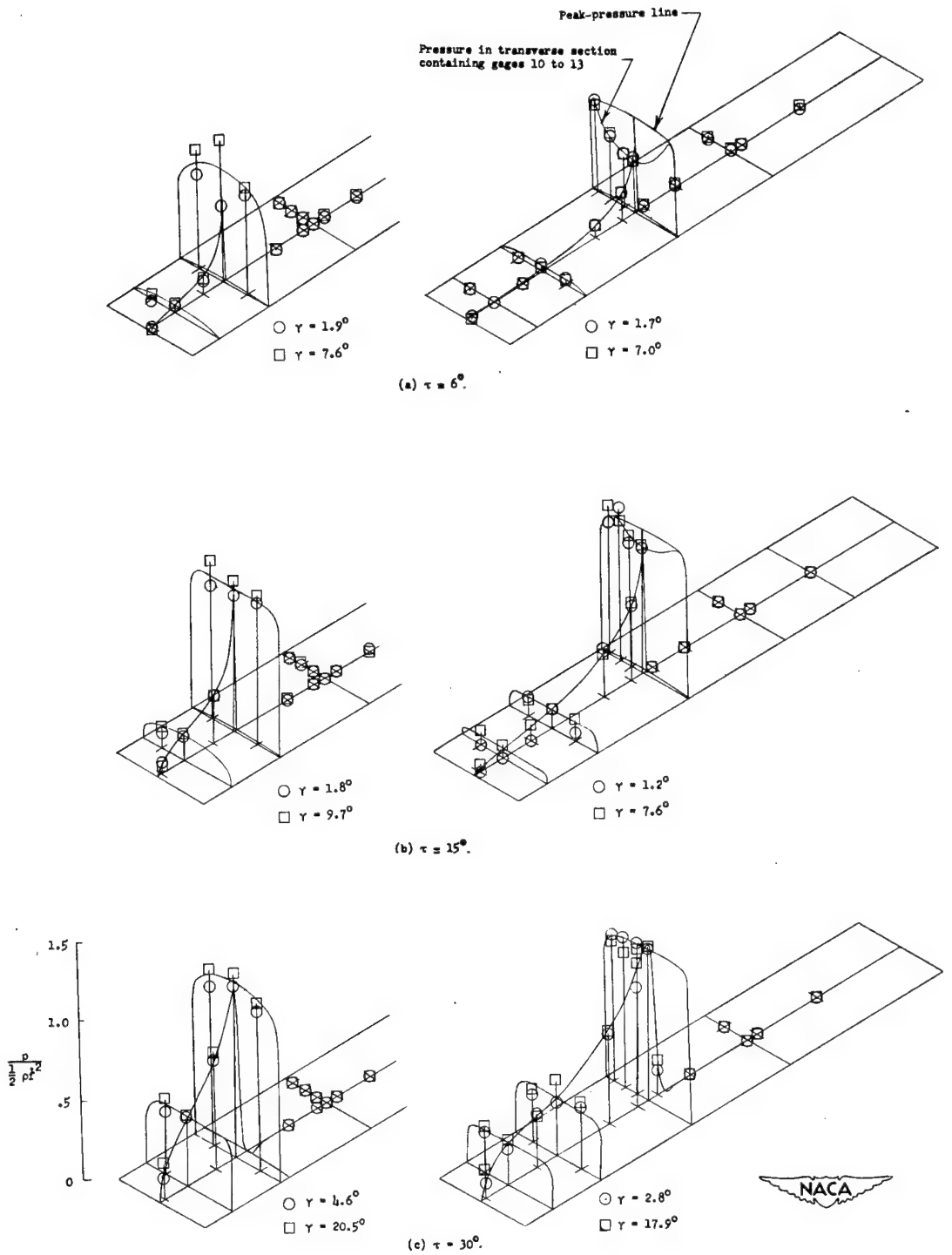

Figure 6.- Effects of flight-path angle on the pressure coefficient $\frac{p}{\frac{1}{2}\rho f^2}$ of the flat plate for various trims and for small and large wetted-length - beam ratios. $C_\Delta = 18.8$.

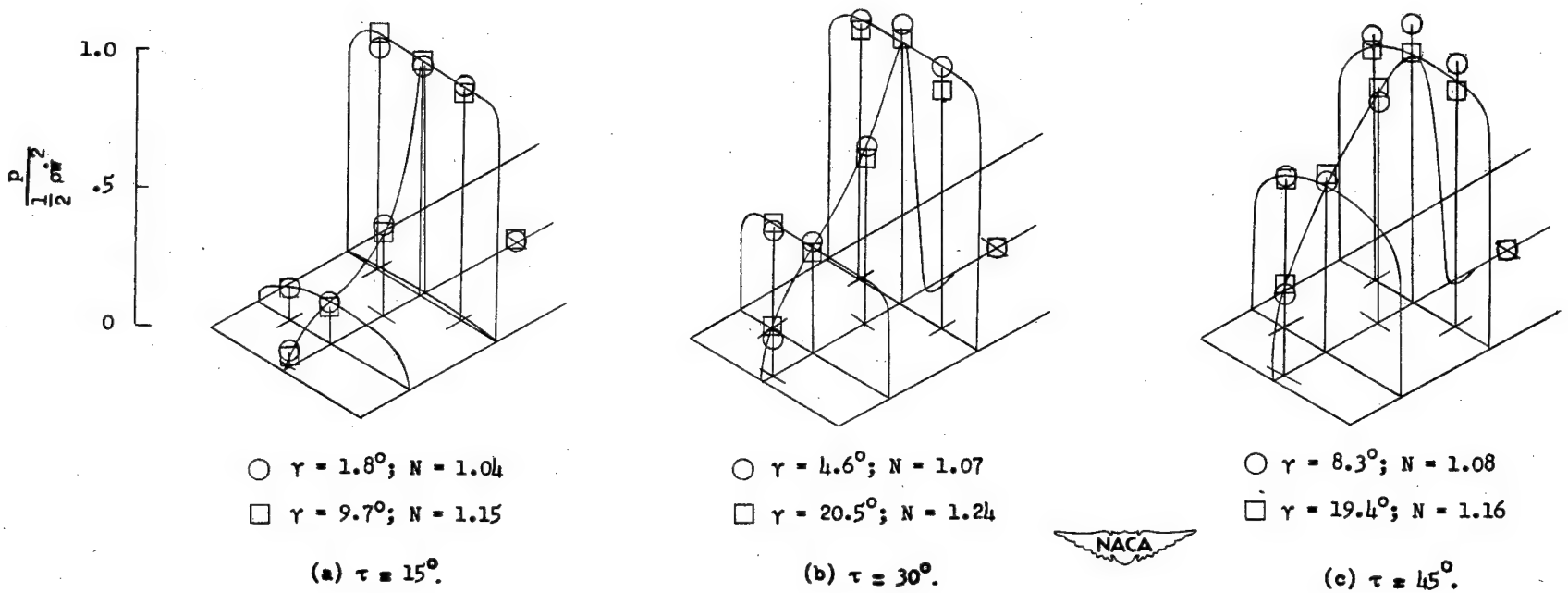

Figure 7.- Effects of flight-path angle on the pressure coefficient $\frac{p}{\frac{1}{2}\rho V^2}$ of the flat plate for various trims and small wetted-length - beam ratios. $C_{\Delta} = 18.8$.

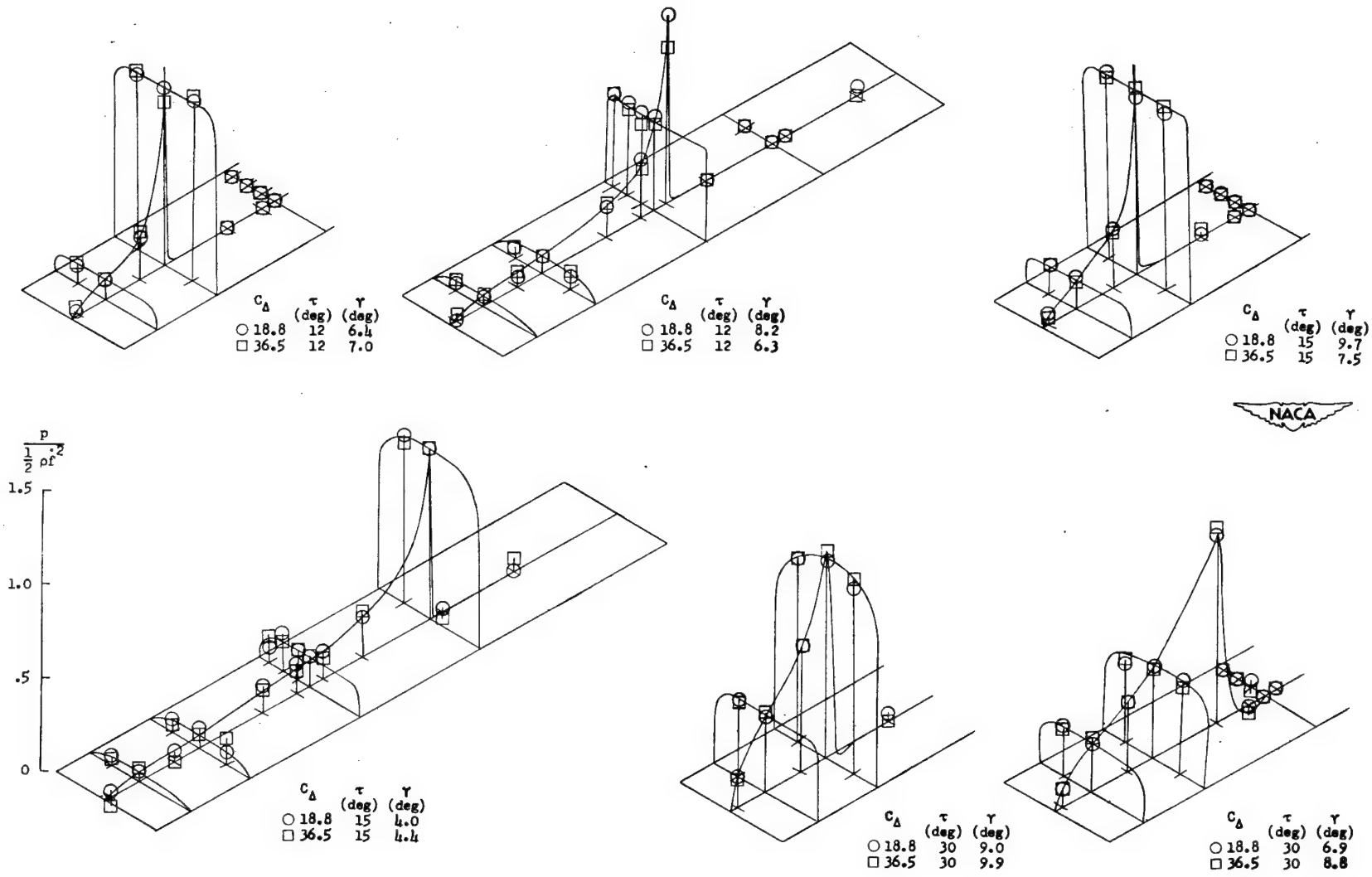

Figure 8.- Comparison of flat-plate pressure coefficients for beam-loading coefficients of 18.8 and 36.5.

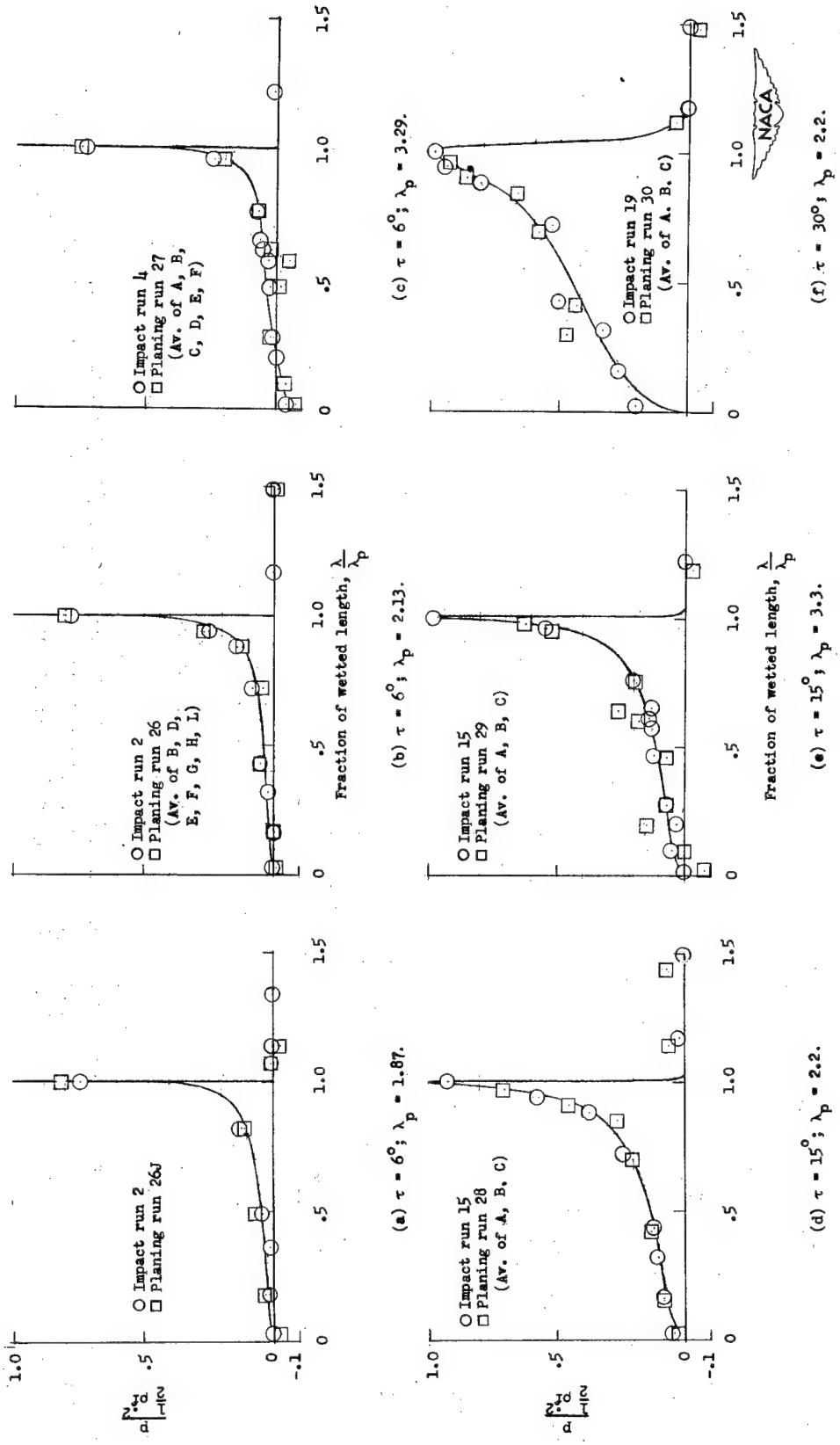

(a) $\tau = 6^\circ$; $\lambda_p = 1.87$.

(b) $\tau = 6^\circ$; $\lambda_p = 2.13$.

(c) $\tau = 6^\circ$; $\lambda_p = 3.29$.

(d) $\tau = 15^\circ$; $\lambda_p = 2.2$.

(e) $\tau = 15^\circ$; $\lambda_p = 3.3$.

(f) $\tau = 30^\circ$; $\lambda_p = 2.2$.

Figure 9.- Comparison of impact and planing pressure coefficients along the center line of the flat plate. (Impact data from table II and planing data from table III.)

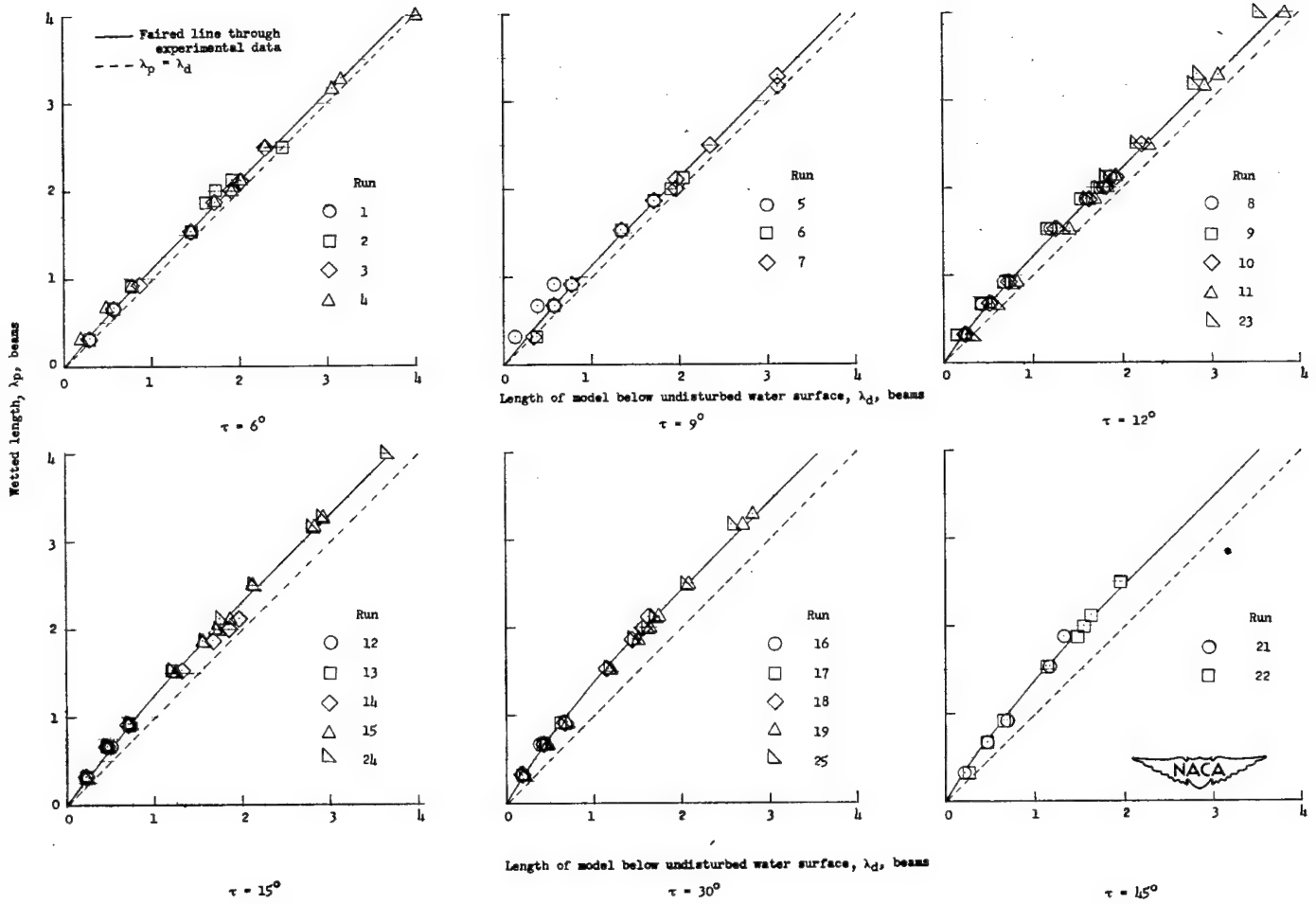

(a) Experimental relationship between the wetted length based on the peak-pressure location and the length of the model below the undisturbed water surface, from variable-resistance slide-wire data in table II.

Figure 10.- Wetted-length relations for the flat plate.

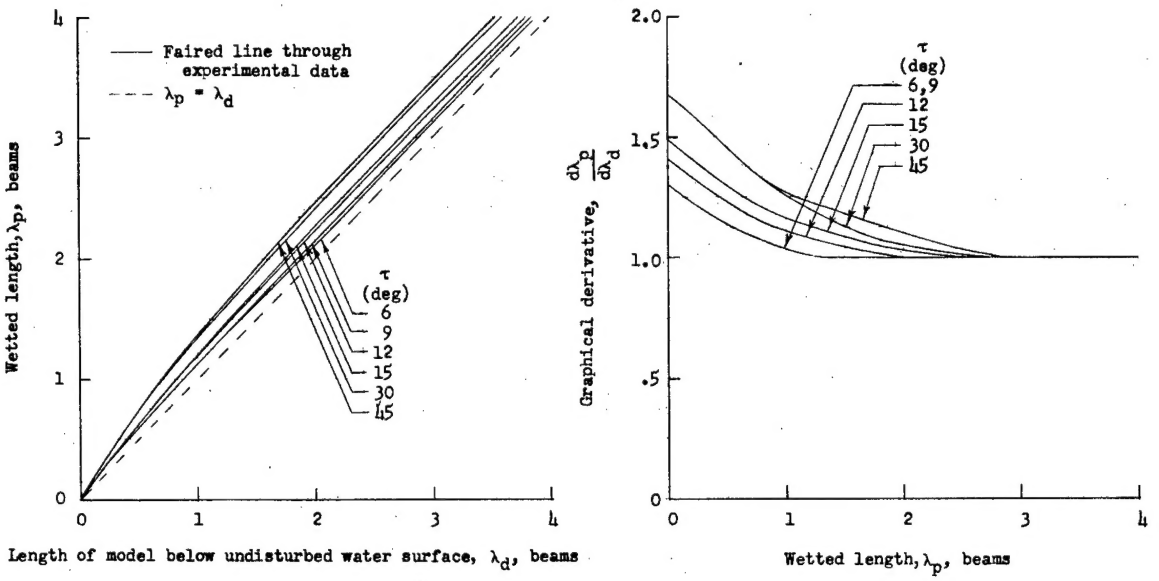

(b) Composite plot of figure 10(a). (c) Graphical derivatives of curves in figure 10(b).

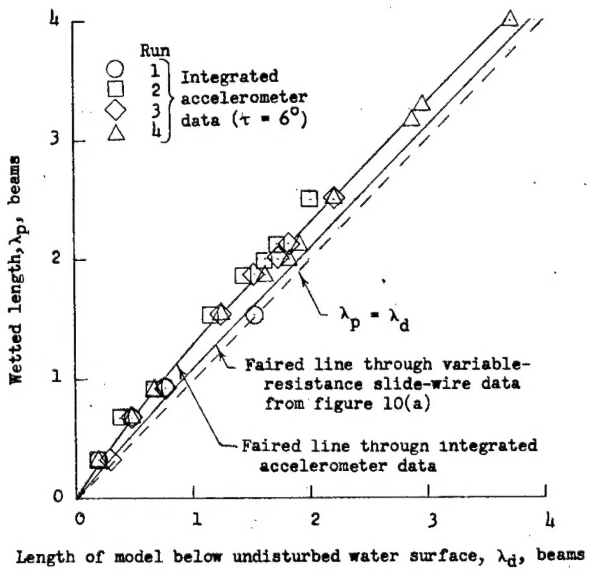

(d) Comparison of wetted lengths obtained by two methods of determining the experimental draft.

Figure 10.- Concluded.

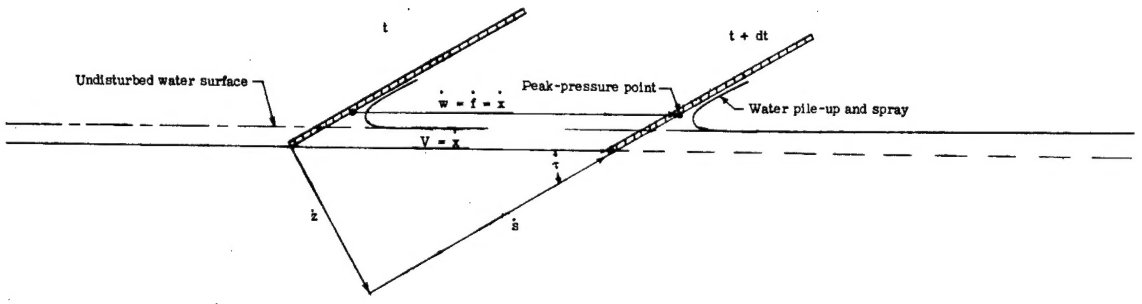

(a) Planing condition.

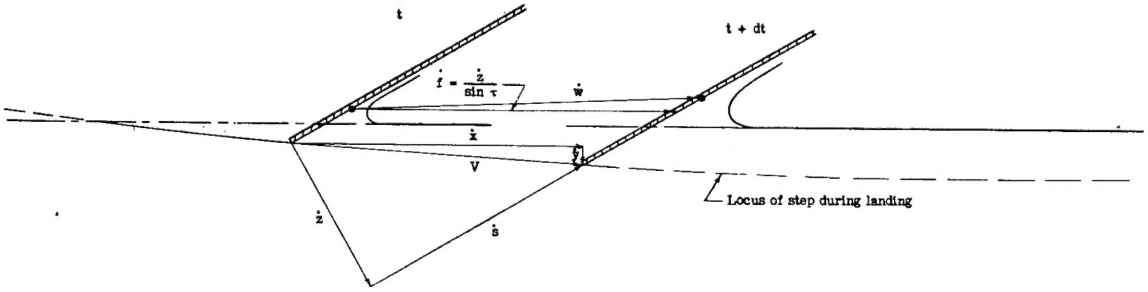

(b) Impact conditions for very small wetted-length - beam ratios.

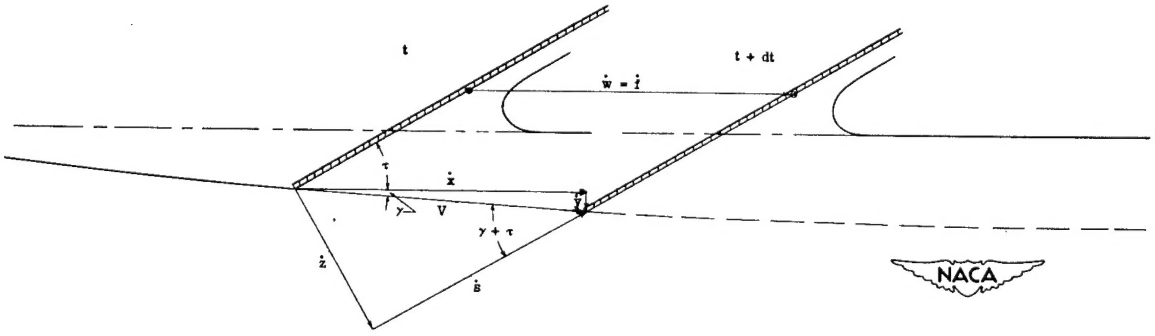

(c) Impact conditions for very large wetted-length - beam ratios.

Figure 11.- Geometrical relations during the planing and the landing of a flat plate.

NACA TN 2453
National Advisory Committee for Aeronautics.
AN EXPERIMENTAL STUDY OF WATER-PRESSURE DISTRIBUTIONS DURING LANDINGS AND PLANING OF A HEAVILY LOADED RECTANGULAR FLAT-PLATE MODEL. Robert F. Smiley. September 1951. 40p. diagrs., 3 tabs. (NACA TN 2453)

Water-pressure, velocity, draft, wetted length, and acceleration measurements are presented for smooth-water landing and planing tests of a rectangular flat-plate model. Landings were made at fixed trims between 6° and 45°, for flight-path angles between 2° and 20°, with beam-loading coefficients of 18.8 and 36.5. Planing runs were made for trims between 6° and 45°. For landings, the experimental pressure coefficients based on the equivalent planing velocity appear to be substantially independent of the deceleration of the model. The peak pressures were approximately equal to the dynamic pressure (over)

Copies obtainable from NACA, Washington

1. Hulls, Seaplane - Length-Beam Ratio (2.3.1)
2. Hulls, Seaplane - Deadrise (2.3.2)
3. Planing Surfaces, Hydrodynamic (2.6)
4. Hydrofoils (2.7)
5. Loads, Landing - Impact, Water (4.1.2.1.2)

I. Smiley, Robert F.
II. NACA TN 2453

NACA TN 2453
National Advisory Committee for Aeronautics.
AN EXPERIMENTAL STUDY OF WATER-PRESSURE DISTRIBUTIONS DURING LANDINGS AND PLANING OF A HEAVILY LOADED RECTANGULAR FLAT-PLATE MODEL. Robert F. Smiley. September 1951. 40p. diagrs., 3 tabs. (NACA TN 2453)

Water-pressure, velocity, draft, wetted length, and acceleration measurements are presented for smooth-water landing and planing tests of a rectangular flat-plate model. Landings were made at fixed trims between 6° and 45°, for flight-path angles between 2° and 20°, with beam-loading coefficients of 18.8 and 36.5. Planing runs were made for trims between 6° and 45°. For landings, the experimental pressure coefficients based on the equivalent planing velocity appear to be substantially independent of the deceleration of the model. The peak pressures were approximately equal to the dynamic pressure (over)

Copies obtainable from NACA, Washington

1. Hulls, Seaplane - Length-Beam Ratio (2.3.1)
2. Hulls, Seaplane - Deadrise (2.3.2)
3. Planing Surfaces, Hydrodynamic (2.6)
4. Hydrofoils (2.7)
5. Loads, Landing - Impact, Water (4.1.2.1.2)

I. Smiley, Robert F.
II. NACA TN 2453

NACA TN 2453
National Advisory Committee for Aeronautics.
AN EXPERIMENTAL STUDY OF WATER-PRESSURE DISTRIBUTIONS DURING LANDINGS AND PLANING OF A HEAVILY LOADED RECTANGULAR FLAT-PLATE MODEL. Robert F. Smiley. September 1951. 40p. diagrs., 3 tabs. (NACA TN 2453)

Water-pressure, velocity, draft, wetted length, and acceleration measurements are presented for smooth-water landing and planing tests of a rectangular flat-plate model. Landings were made at fixed trims between 6° and 45°, for flight-path angles between 2° and 20°, with beam-loading coefficients of 18.8 and 36.5. Planing runs were made for trims between 6° and 45°. For landings, the experimental pressure coefficients based on the equivalent planing velocity appear to be substantially independent of the deceleration of the model. The peak pressures were approximately equal to the dynamic pressure (over)

Copies obtainable from NACA, Washington

1. Hulls, Seaplane - Length-Beam Ratio (2.3.1)
2. Hulls, Seaplane - Deadrise (2.3.2)
3. Planing Surfaces, Hydrodynamic (2.6)
4. Hydrofoils (2.7)
5. Loads, Landing - Impact, Water (4.1.2.1.2)

I. Smiley, Robert F.
II. NACA TN 2453

NACA TN 2453
National Advisory Committee for Aeronautics.
AN EXPERIMENTAL STUDY OF WATER-PRESSURE DISTRIBUTIONS DURING LANDINGS AND PLANING OF A HEAVILY LOADED RECTANGULAR FLAT-PLATE MODEL. Robert F. Smiley. September 1951. 40p. diagrs., 3 tabs. (NACA TN 2453)

Water-pressure, velocity, draft, wetted length, and acceleration measurements are presented for smooth-water landing and planing tests of a rectangular flat-plate model. Landings were made at fixed trims between 6° and 45°, for flight-path angles between 2° and 20°, with beam-loading coefficients of 18.8 and 36.5. Planing runs were made for trims between 6° and 45°. For landings, the experimental pressure coefficients based on the equivalent planing velocity appear to be substantially independent of the deceleration of the model. The peak pressures were approximately equal to the dynamic pressure (over)

Copies obtainable from NACA, Washington

1. Hulls, Seaplane - Length-Beam Ratio (2.3.1)
2. Hulls, Seaplane - Deadrise (2.3.2)
3. Planing Surfaces, Hydrodynamic (2.6)
4. Hydrofoils (2.7)
5. Loads, Landing - Impact, Water (4.1.2.1.2)

I. Smiley, Robert F.
II. NACA TN 2453

NACA TN 2453

corresponding to the velocity of the peak-pressure point.

Copies obtainable from NACA, Washington

NACA TN 2453

corresponding to the velocity of the peak-pressure point.

Copies obtainable from NACA, Washington

NACA TN 2453

corresponding to the velocity of the peak-pressure point.

Copies obtainable from NACA, Washington

NACA TN 2453

corresponding to the velocity of the peak-pressure point.

Copies obtainable from NACA, Washington